NUMERICAL EXPERIMENTS AND THEORETICAL ANALYSIS

ON THE SOURCES OF IRREVERSIBILITY IN MECHANICAL SYSTEMS

A THESIS

Presented to

The Faculty of the Division of Graduate

Studies and Research

by

Spotswood Douglas Stoddard, Jr.

In Partial Fulfillment

of the Requirements for the Degree

Doctor of Philosophy in the

School of Physics

Georgia Institute of Technology

February, 1973

NUMERICAL EXPERIMENTS AND THEORETICAL ANALYSIS

ON THE SOURCES OF IRREVERSIBILITY IN MECHANICAL SYSTEMS

Approved:

Chairman

Date approved by Chairman: February 28, 1973

ACKNOWLEDGMENTS

I would like to thank Professor Joseph Ford for his considerable help and encouragement in the course of this work. That my wife, Phyllis, and daughter, Margaret Ann, have survived the last five years is alone worthy of mention, their positive contributions notwithstanding.

I must also express my gratitude to the Physics faculty for the financial support provided by their occasionally inviting me to the faculty poker game.

TABLE OF CONTENTS

TABLE OF CONTENTS (Continued)

LIST OF TABLES

LIST OF ILLUSTRATIONS

SUMMARY

The basic problem treated by Boltzmann and Gibbs involved obtaining a workable theory describing irreversible and equilibrium thermodynamic behavior starting from reversible microscopic dynamics. Their theory leaned heavily on the plausible but unproven hypothesis of ergodicity, which, loosely speaking, asserts that each trajectory of an isolated system samples the entire energy surface of that system. They deduced that an essentially irreversible approach to equilibrium followed from the ergodic hypothesis, despite the reversibility of the under-lying microscopic dynamics. Until recently, the ultimate justification for introducing the ergodic assumption has been empirical verification of the final predictions made by the Boltzmann-Gibbs theory. Perhaps the most definitive of the recent evidence supporting the ergodic assumption has been provided by Sinai. In particular, assuming only the validity of Newton's equations of motion, Sinai has rigorously estab-lished that a hard-sphere gas does indeed exhibit the ergodic behavior hypothesized by Boltzmann and Gibbs. For the purposes of this work, the key feature of Sinai's proof lies in his showing ergodicity to follow from the fact that the distance between almost any two system trajec-tories initially close together in phase space grows exponentially with time.

It is believed that Sinai's proof can be extended to a large class of systems having purely repulsive interparticle forces, but there is doubt concerning the extension of the theorem to systems having

attractive as well as repulsive forces. Thus in this research we
chose to study a Lennard-Jones gas system empirically on a computer in
order to investigate the question of ergodicity for a physically real-
istic system having attractive as well as repulsive interparticle
forces. These computer experiments show that trajectories for this
Lennard-Jones system separate exponentially in time at the temperatures
(total system energies) studied. According to the theory of Sinai, as
well as that of Arnold and Sinai, this empirical evidence for exponen-
tially separating trajectories implies that the Lennard-Jones system
is ergodic, as is the hard-sphere gas.

The computer experiments also lend themselves to the testing of
an hypothesis in the field of kinetic theory. In kinetic theory, diver-
gences appear when transport coefficients are calculated as series
expansions in the system density. The calculation assumes that binary
collisions are the dominant transport mechanism at low density, with
three-body, four-body, etc., collisions becoming important sequentially
as the density is increased. Our hypothesis involved the conjecture
that this sequential assumption might be in error and that cooperative
behavior--collisions among large numbers of particles--might sud-
denly appear as the density increased, thereby destroying the conver-
gence of the terms in the series expansions. It was expected that the
onset of cooperative behavior would cause the trajectory exponentiation
rate to exceed considerably the exponentiation rate due to binary col-
lisions alone.

In order to test our hypothesis, a theory of trajectory-
exponentiation in a hard-sphere gas was developed. This theory yielded

an expression for the rate of exponentiation due to binary collisions alone, because many-particle collisions, and hence cooperative effects, were suppressed by the theoretical calculation. Contrary to our hypothesis, the empirically-observed exponentiation rate for the Lennard-Jones gas was in reasonable agreement with the theoretically-derived binary collision expression over the entire range of densities studied. Indeed, this agreement extended to densities sufficiently high that three-body and four-body collisions were observed in the Lennard-Jones gas. Since no cooperative behavior was needed to explain the trajectory exponentiation rates, even at these relatively high densities, no empirical support was obtained for the conjecture linking divergences in transport coefficients with cooperative behavior.

CHAPTER I

INTRODUCTION

This dissertation presents the results of some numerical
experiments executed on a digital computer and a theoretical analysis
that partially predicts these results. From the numerical experiments,
which consist of the numerical integration of Hamilton's equations, it
is shown that a classical Lennard-Jones gas system exhibits exponential
growth of the separation distance between trajectories in phase space
as the system evolves in time; and data is obtained on the exponential
growth rate over a range of macroscopic equilibrium conditions. This
behavior is explained by a theoretical treatment consisting of an anal-
ysis of the binary collision process.

Motivation

This study was motivated by two distinct considerations. First,
the ergodic assumptions of Boltzmann and Gibbs[1] can be shown[2] to hold
rigorously for systems in which the phase-space trajectories separate
exponentially with time, but there are tremendous technical difficulties
in mathematically proving that a given system has this exponential
character. At present, it has not been shown that systems with attrac-
tive interparticle forces exhibit exponentially separating trajectories.
In this work, the exponentially separating character of trajectories
for an attractive-force, Lennard-Jones gas system is demonstrated empir-
ically by means of a digital computer.

Second, the conjecture was made that the term-by-term divergences which arise in the contemporary kinetic theory of transport coefficients[3] could be related to an abrupt appearance of cooperative behavior among all the particles of the system as the density increased. We undertook to prove or disprove this conjecture by searching for a more rapid increase in the exponential growth rate with density than could be explained by binary collision processes alone.

In the remainder of this chapter the background material and objectives are given in more detail.

Ergodic Theory

The problem of statistical mechanics is to develop a theory for the irreversible and equilibrium behavior of macroscopic systems start-ing from reversible microscopic dynamics. Boltzmann and Gibbs were the first to do this,[1,4-7] although their treatments included assumptions which have been put on a rigorous basis only recently by modern ergodic theory.[2,8-12] In this section, only those features of the original Boltzmann-Gibbs theory or the more recent ergodic theory having a direct bearing on our work are presented. The discussion generally follows Uhlenbeck and Ford[5] and Wightman.[11] For a more detailed exposition the reader is referred to the references.[1,2,4-12]

Let us begin by considering the reversible, microscopic dynamics of an isolated mechanical system of N particles. Here the state (micro-state) of an isolated system is represented by a point in the phase space (Γ-space) of the system. This representative point moves in time along a phase-space trajectory specified by a solution of the dynamical

equations of motion. Indeed, a detailed, general solution of the
equations of motion would allow a determination of all possible trajec-
tories and would therefore provide all possible physical information
about the system; however, it is not feasible to obtain such a general
solution or its associated trajectories for any but the simplest mechan-
ical systems. Thus, in attempting to provide a method for calculating
equilibrium, macroscopically observable quantities, statistical mechan-
ics was forced to devise a scheme which avoids having to solve the
equations of motion. It was possible to devise such a scheme because
the macroscopically observable quantities are insensitive to the precise
microscopic mechanical state of the system. These equilibrium quanti-
ties can be shown to be time averages of certain phase functions, that
is, certain functions of the microscopic variables (q,p), where q and p
are the generalized coordinates and momenta of the system. To calculate
these time averages would require knowledge of the detailed solutions
of the equations of motion. Since such knowledge is not available,
statistical mechanics sought to replace these time averages by some
equivalent but more easily calculated averages.

Boltzmann was the first to make such a replacement successfully.
He introduced various plausibility arguments in support of the hypothe-
sis (ergodic hypothesis) that the representative point of a system in
phase space wanders freely over the energy surface, spending equal times
in equal (hyper-) areas. On the basis of the ergodic hypothesis,
Boltzmann then argued that the equilibrium values of macroscopic quan-
tities could be calculated be averaging the appropriate phase functions
over the energy surface rather than over a time interval. In this

fashion, Boltzmann used the ergodic hypothesis to ease the calculation of macroscopically observable quantities for systems at equilibrium.

Ergodicity also appears in Boltzmann's view of the approach to equilibrium. Since the long-time average of a phase function is presumed to equal the measured value of the corresponding observable quantity for a system at equilibrium, Boltzmann argued that most microstates (values of the microscopic variables (q,p)) on a freely-wandering, ergodic trajectory must correspond to the same thermodynamic equilibrium state. As a consequence, he suggested that most microstates on the entire energy surface correspond to a single macroscopic equilibrium state. Therefore, Boltzmann expected that an isolated system started in some disequilibrium state and subsequently allowed to follow its assumed ergodic tendency to wander freely over the energy surface would surely approach equilibrium because most microstates on the energy surface correspond to the equilibrium state.

Gibbs[6] restated and generalized Boltzmann's arguments by introducing an ensemble--a collection of representative system points in phase space confined for our purposes to a thin energy shell. The phase function that gives the density of representative system points in an ensemble is called the distribution of the ensemble. Usually one normalizes this distribution to unity and treats it as a probability distribution. This treatment is allowable because, in the course of time, the representative system points of an ensemble move like an incompressible fluid on the energy shell, according to the Liouville theorem.[4]

A physically observable system state (macrostate) corresponds to a large number of microstates. Therefore, by a physical measurement one

determines the region on the energy shell wherein the representative point of a system must lie, but not in which of the possible micro-states it exists. As there is no a priori reason to assign any one of the possible microstates in preference to another, a system prepared in a given macrostate is represented by an ensemble with a distribution that is initially zero outside and constant inside the appropriate energy shell region. As the system evolves from the prepared state, the corresponding distribution can change its shape but not its volume. Gibbs suggested that such a distribution evolves in time into a long, thin filament which eventually permeates the energy shell uniformly. At any time in the process, one considers the probability that the original system has evolved to some particular macrostate to be the measure of the part of the distribution which then occupies the region of the energy shell associated with that macrostate. When the distri-bution becomes uniform over the energy shell, the probability of a particular final macrostate is proportional to the (hyper-) volume of the corresponding region. Because by far the largest volume belongs to a single macroscopic equilibrium state, this state is overwhelmingly likely to be the final one. The "extension-in-phase" of Gibbs gives the same final results as the ergodic hypothesis of Boltzmann, both in the ultimate approach to equilibrium and in the replacement of time averages by phase space averages.

The rigorous ergodic theorems of Birkhoff[11] allowed Boltzmann's assumptions about isolated systems to be expressed in terms of suffi-cient conditions. These theorems are: 1) the time average of an integrable phase function exists on almost every trajectory, and 2) for

metrically transitive systems, the time average is the same on almost
every trajectory and is equal to the uniformly weighted phase space
average of the phase function. We use the term "almost" in the sense
of measure theory to mean "except for a set of measure zero." A
mechanical system is said to be metrically transitive if it is impos-
sible to divide the energy surface into two regions of positive measure
such that almost all trajectories beginning in one of the regions remain
there. The modern terminology is to call metrically transitive systems
ergodic, and we shall follow this practice.

Although ergodicity in the preceding sense is sufficient to
insure the equality of time and phase-space averages, there are stronger
conditions of stochasticity which also ensure the equality of time and
phase-space averages;[2] we shall consider two of these, the first being
the property of mixing.

Since a distribution of points on the energy surface moves like
an incompressible fluid, there exists an invariant measure there, which
we shall call μ. Suppose that the measure of the entire surface is nor-
malized to unity. Let A be a fixed set on the surface, and let B_t be
a set on the surface at time t that has evolved from an original set B_o
at time t=0 according to the dynamics of the system. The system is
then said to be mixing if we have

$$\lim_{t \to \infty} \mu(A \cap B_t) = \mu(A)\mu(B_o) . \tag{1}$$

It can be shown[2] that mixing implies ergodicity, but the converse is
not true.

We now give an example (adapted from Arnold and Avez[2]) illustrating the mixing property: suppose that we have a glass containing 80 per cent Coca-Cola and 20 per cent rum. If B_o is the region in the glass originally occupied by the rum, then after sufficient stirring ($t \to \infty$) any set A somewhere in the glass would be expected to consist of Coca-Cola and rum in four-to-one proportions. This is exactly the behavior indicated by Eq. (1).

Comparison of the last three paragraphs with the arguments of Boltzmann and Gibbs reveals that mixing is similar to Gibbs's picture while ergodicity (metric transitivity) is closer to the ideas of Boltzmann.

The second stochastic property we shall need is that exhibited by a class of systems known as C-systems.[2,11,12] These systems will be discussed in more detail in the next chapter; for the present, let us note that C-systems have the following characteristic behavior: every element of area on an energy surface of a C-system changes shape as it moves under the dynamical equations of motion in such a way that it expands exponentially in at least one direction and contracts exponentially in at least one other. Intuitively one can see that such behavior leads to a distribution of points on the energy surface being drawn out into a filament as discussed by Gibbs, and in fact it can be shown[2] that C-systems are ergodic and mixing. For our work, C-systems have the additional advantage that their behavior is relatively easy to characterize empirically in computer studies.

Sinai[12] has shown that a hard-sphere gas is ergodic and mixing and exhibits exponential behavior similar to that of a C-system.

Further, Wightman[11] states that the "folklore" holds Sinai's results

to be extendable to a large class of purely repulsive forces but that

attractive forces would introduce stable, periodic orbits at low enough

energies, thus preventing ergodic behavior. A natural question to ask

is then the following one: do systems with attractive interparticle

forces exhibit this exponential behavior? This is one of the questions

which we answer here empirically.

Dense Gases

Another motivating factor in our research lies in the work of

Miller,[13] who performed some computer studies on stellar dynamical

systems and observed exponential behavior as described in the preceding

section. He concluded that his results indicated cooperative behavior

among all of the particles because the results deviated from that

expected due to binary collisions alone. This behavior was attributed

to the long range of the gravitational force. We were led by this con-

clusion to make the conjecture that cooperative behavior might make a

sudden appearance as the density increased in a system having short-

range interparticle forces. If it did so, one might then, in terms of

this behavior, explain the divergences that occur when transport coeffi-

cients are calculated by means of a series expansion in powers of the

density. In particular,[3] this calculation assumes that binary (two-

particle) collisions are the dominant mechanism for transport phenomena

at low densities and that three-body, four-body, etc., collisions

become important sequentially as the density increases. The sudden

appearance of cooperative behavior among many particles would indicate

that this sequential assumption was not valid but rather that a sudden transition from two-body to many-body behavior occurred. As was mentioned earlier, we observed exponential behavior in the system studied, and we expected to detect such a transition, if any, by looking for a sudden, rapid increase in the exponential growth rate as the density was increased.

We did not observe the onset of cooperative behavior. Nevertheless, this was the motivation for our study of the gas system over the wide density range that was covered by our experiments. The major motivation of the theoretical analysis that will be reported was to determine the exponential growth rate due to binary collisions alone in order to compare it to the experimental growth rate.

In summary, our research consists of computer experiments designed to detect exponential behavior in a certain gas system and to gather data on the exponential growth rate over a wide density range. It further consists of a theoretical analysis to which the computer results can be compared. These things were undertaken to provide empirical support for some of the basic postulates of statistical mechanics and to attempt to account for some difficulties in the kinetic theory of dense gases.

CHAPTER II

INTRODUCTION TO THE NUMERICAL EXPERIMENTS

This chapter contains an introductory description of the numerical experiments mentioned in the preceding chapter. The following chapter then gives a theoretical calculation of some of the quantities observed in these experiments. By "observed" we shall always mean "computed in the course of numerical experiments" throughout this thesis. In still later chapters we shall give a presentation of the experimental results and a comparison between experiment and theory. This order of presentation is followed because the theoretical calculation uses quantities defined in the description of the experiments, and the experimental results are then presented in terms of theoretically derived quantities to facilitate comparison.

In the next section we develop some notation and define a C-system more precisely than before. The weight of the empirical evidence presented later is that the gas system under consideration is a C-system.

Mathematical Preliminaries

A classical system of M degrees of freedom is described by giving its generalized coordinates q_i and their conjugate momenta p_i, where $i = 1,\ldots,M$. The state of such a system at any instant of time t is conveniently represented by a phase space point $(q,p) = (q_1,\ldots,q_M, p_1,\ldots,p_M)$ in the 2M-dimensional, Euclidean phase space having the q_i and p_i as coordinate axes. The representative point moves along a

trajectory in phase space as the system evolves in time. The time
evolution of the system is uniquely generated from the Hamiltonian
$H(q,p)$ by means of Hamilton's equations of motion:

$$\frac{dq_i}{dt} = \frac{\partial H}{\partial p_i} \ , \tag{2}$$

$$\frac{dp_i}{dt} = - \frac{\partial H}{\partial q_i} \ , \tag{3}$$

where $i = 1,\ldots,M$.

We shall restrict our attention to Hamiltonians $H(q,p)$ which are
not explicit functions of the time and which yield trajectories lying
totally within a bounded region of phase space. We have $dH/dt = 0$ since
$H(q,p)$ does not depend explicitly on the time; therefore each trajectory
is restricted to lie on an energy surface given by[14]

$$H(q,p) = E \ , \tag{4}$$

where E is the total energy of the system. The energy surface is a
(2M-1)-dimensional sub-space of the phase space and has finite, (2M-1)-
dimensional (hyper-) area since the system motion is bounded.

Let us denote a single phase space point by $y = (q,p)$, and let
$y(t) = (q(t), p(t), -\infty < t < \infty)$ be a parametric representation of a
trajectory. Suppose the trajectory $y(t)$ passes through the point y_0 at
the time $t = 0$. In the energy surface containing $y(t)$, construct the
(2M-2)-dimensional (hyper-) plane normal to $y(t)$ at y_0. Let δy_0 repre-
sent a small displacement from y_0 lying in the normal plane, y_0' the
point $y_0 + \delta y_0$, $y'(t)$ the trajectory through y_0', and $\delta y(t)$ the

difference $[y'(t) - y(t)]$ at any time t.

A system is said to be a C-system if the normal plane can be split into exactly two sub-spaces, called the dilating and contracting spaces, each sub-space having dimensionality one or higher, and further, if there exists a positive λ (which may depend on y_o) such that the following inequalities hold:

$$|\delta y(t)| \gtreqless e^{\lambda t} |\delta y_o| , \qquad t \gtreqless 0 , \qquad (5a)$$

$$|\delta y(t)| \lesseqgtr e^{\lambda t} |\delta y_o| , \qquad t \lesseqgtr 0 , \qquad (5b)$$

for δy_o in the dilating space, and

$$|\delta y(t)| \lesseqgtr e^{-\lambda t} |\delta y_o| , \qquad t \gtreqless 0 , \qquad (6a)$$

$$|\delta y(t)| \gtreqless e^{-\lambda t} |\delta y_o| , \qquad t \lesseqgtr 0 , \qquad (6b)$$

for δy_o in the contracting space. Conditions (5) or (6) are required to be valid for arbitrarily large $|t|$ only for sufficiently small $|\delta y_o|$. There must exist some displacements δy_o for almost every point on the energy surface such that these conditions hold. It can be shown[2] that C-systems are mixing and ergodic. Therefore, a system exhibiting exponential behavior of this type for almost all trajectories would be expected to possess all of the statistical properties hypothesized by Boltzmann and Gibbs.

From the C-system definition, the dilating space has dimensionality one or more; thus, the entire contracting space has measure zero in the normal plane, and conversely, so does the dilating space. Consequently, almost all $\delta y(t)$ will be dominated by Eq. (5a) for $t \to +\infty$ and by

Eq. (6b) for t → -∞. Our experimental evidence indicates that in our case

this asymptotic behavior is established virtually immediately (see

Figures 3 through 11). We shall use Eq. (5a) exclusively as our exper-

imental criterion for C-system behavior since we have integrated the

equations of motion only in the forward time direction, starting from

some specified initial conditions.

Throughout the rest of this thesis, we shall use the term

"exponentiation rate" for the coefficient of an independent variable in

the exp function, e.g., λ in Eq. (5a), and the term "exponentiation of

trajectories" for the conditions indicated by Eqs. (5) and (6).

Description of the Gas System

The gas system investigated was a mathematical model of an inert

gas. We attempted to make the model as realistic as possible, within

the limitations of classical mechanics and of computer time.

The system consisted of N point particles each having mass m.

For various reasons which will be described presently, the system was

restricted to two spatial dimensions; each particle was confined to

move within the same bounded, two-dimensional area. We denote the two-

dimensional position vector of the ith particle as $\vec{r}_i$, and the corre-

sponding momentum vector as $\vec{p}_i = m\, d\vec{r}_i/dt$.

Potential

We chose a Lennard-Jones pair potential for the gas system

because this interaction is supported by both theoretical[15] and experi-

mental[16] evidence. The potential was modified slightly to have a

finite range for convenience in the computer calculations. In terms of

the Euclidean, two-dimensional distance r between two particles, the range r_c of the interaction, and the tabulated[16] Lennard-Jones parameters ϵ and σ, the pair potential U is given by

$$U(r) = 4\epsilon \left\{ \left(\frac{\sigma}{r}\right)^{12} - \left(\frac{\sigma}{r}\right)^{6} \right.$$

$$\left. + \left[6\left(\frac{\sigma}{r_c}\right)^{12} - 3\left(\frac{\sigma}{r_c}\right)^{6} \right] \left(\frac{r}{r_c}\right)^{2} - 7\left(\frac{\sigma}{r_c}\right)^{12} + 4\left(\frac{\sigma}{r_c}\right)^{6} \right\} \qquad (7)$$

when $r < r_c$, and is zero when $r \geq r_c$. We note that both U of Eq. (7) and dU/dr go continuously to zero as r approaches r_c and that U differs only slightly from the precise Lennard-Jones potential when r_c is taken to be several times the size of σ. In our experiments we set $r_c = 5\sigma$. The potential, as used in our experiments, is plotted in Figure 1.

It was convenient in our computer experiments to express distance in units of σ, energy in units of 4ϵ, and mass in units of m. In terms of these units, Eq. (7) for U becomes

$$U(r) = \frac{1}{r^{12}} - \frac{1}{r^{6}} + \left(\frac{6}{r_c^{12}} - \frac{3}{r_c^{6}} \right)\left(\frac{r}{r_c}\right)^{2} - \frac{7}{r_c^{12}} + \frac{4}{r_c^{6}} . \qquad (8)$$

With Eq. (8), the full Hamiltonian H for our N-particle system may be written as

$$H = \sum_{i=1}^{N} \frac{P_i^2}{2} + \sum_{i>j} U(r_{ij}) , \qquad (9)$$

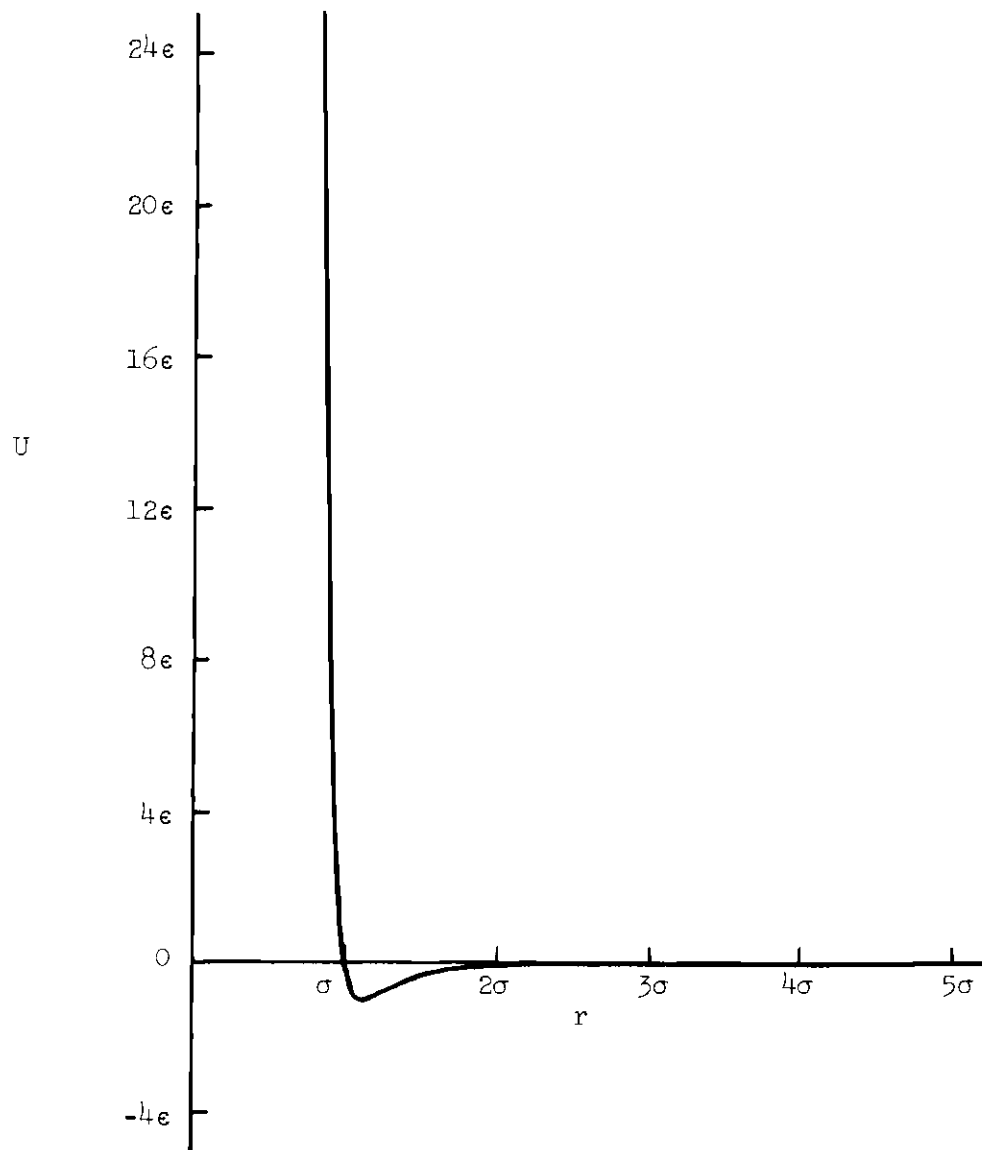where the distance r_{ij} between particles i and j is given by

Figure 1. Cut-Off Lennard-Jones Potential.

$$r_{ij} = |\vec{r}_i - \vec{r}_j| \tag{10}$$

Dimensionality

Although some of our initial computer work was done on a three-dimensional gas, by far the largest amount was done for gas particles moving in only two dimensions. There were several reasons for this, the primary one being to achieve faster computer operation without loss of significant generality. In addition, a two-dimensional system of the type used in these investigations has fewer particles near the boundaries than a three-dimensional system with the same number of particles; thus the boundary conditions have less effect on a two-dimensional system. Moreover, the theoretical development which we shall present later would have been somewhat more complicated in three dimensions with little promise of adding enough additional information to justify the effort. Finally, we expect the qualitative features to be the same in the simpler, two-dimensional system as in the more physically realistic three-dimensional one since the most important source of exponentiating trajectories for gas systems is the binary collision process[2,13] which is identical in two and three dimensions.

Boundary Conditions

In preliminary experimentation with various types of reflecting walls for the system, it was found that such walls contributed in a significant and unpredictable way to the exponentiation rate being observed. It was therefore decided to eliminate the walls altogether by using periodic boundary conditions. With these boundary conditions, the exponentiation rate is determined by the effects of interactions among the particles alone.

The system with periodic boundary conditions was laid out in the shape of a square, the opposite edges of which were effectively joined so a particle leaving the system through one edge of the square immediately re-entered through the opposite edge. The potential was also effective across the boundaries; thus, our system had the topology of a torus. Systems with this topology have frequently been the subject of studies in ergodic theory.[2]

Description of the Numerical Experiments

As has been indicated earlier, the numerical experiments described in this section were performed to obtain evidence that the trajectories exponentiate in gas systems having attractive interparticle forces and to gather data on the exponentiation rate over a range of densities.

Experimental Procedure

The experimental procedure was essentially the same as Miller's procedure.[13] A fourth-order, variable-step Runga-Kutta method[17] was used for all numerical integrations.

In our terminology, a single experiment consisted of integrating Hamilton's equations of motion simultaneously for two macroscopically identical systems. The representative points in phase space for the systems were initially separated by a very small distance (on the order of 10^{-7} in the units of Eq. (8)). The equations of motion were then integrated until the distance between the representative points grew by several orders of magnitude.

Two groups of such experiments were run. For the first and by far the largest group, the density was varied and the temperature held

approximately constant. For the much smaller second group, the temperature was varied at constant density. The number of particles was held constant at $N = 100$ in both groups of experiments.

Observed Quantities

It was mentioned previously that the major observed quantity in our experiments was the exponentiation rate of the trajectories. For any single experiment, however, the trajectories separated exponentially only on the average (see Figures 3 through 11); it was therefore necessary to compute a time-averaged exponentiation rate. In order to make such a computation, we experimentally obtained the distance between the trajectories as a function of time. For the purpose of preserving dimensional homogeneity, the distances D_p in configuration space and D_p in momentum space were defined separately at time t as

$$D_q(t) = \sqrt{\sum_{i=1}^{N} [\vec{r}_i'(t) - \vec{r}_i(t)]^2} \; , \tag{11}$$

$$D_p(t) = \sqrt{\sum_{i=1}^{N} [\vec{p}_i'(t) - \vec{p}_i(t)]^2} \; , \tag{12}$$

where we use a prime (') to distinguish the second system from the first. The experimental values for these distances were then plotted in the form of $\log_{10} D_q$ and $\log_{10} D_p$ versus time. The resulting graphs yielded approximately straight lines which were then fitted by a least-squares method to obtain time-averaged values for the exponentiation rates λ_q and λ_p defined by

$$\lambda_q = \frac{d\langle \log_{10} D_q \rangle}{dt} , \qquad (13)$$

$$\lambda_p = \frac{d\langle \log_{10} D_p \rangle}{dt} , \qquad (14)$$

where the angular brackets here indicate the least-squares derived quantities.

The results may be conveniently interpreted by expressing the exponentiation rates with respect to the number of collisions that have occurred up to time t instead of with respect to t itself. In order to do this, collisions were counted as they occurred during the integration process. At high enough density in a real gas one would expect three-body and higher-order collisions to occur, and we observed such collisions in the model.

For the purpose of counting, an n-body collision was defined as the formation and subsequent dissolution of a group of n particles. A group was defined as a collection of particles such that each member of the group was within a given distance of at least one other member. In our experiments we took this distance to be σ of Eq. (7). A collision was counted when the first particle left a group, but not when successive particles did, unless a new particle joined the group before the group became completely broken up. In this latter case a new collision was counted when the first particle left the new group, and so on.

In this chapter the experimental procedure has been described only so far as necessary to motivate and introduce the theoretical discussion of the following chapter. We shall return to the description of the

experiments and the presentation of the data after we have obtained some
theoretical results for comparison.

CHAPTER III

THEORETICAL ANALYSIS

The objective of the theory discussed in this chapter is to predict the exponentiation of trajectories in a gas system and to derive an expression for the exponentiation rate which may be compared with experiment. The following derivation is concerned exclusively with binary collision processes, even though higher-order collision processes were observed empirically. This restriction to binary collisions was made because a major aim of our experiments was to find in what way the observed exponentiation differed from purely binary collision behavior as the density increased. It therefore behooved one to determine what this purely binary behavior might be.

The theoretical discussion considers two macroscopically identical systems which have representative points initially only slightly separated in phase space, just as in the experiments. We focus our attention on a single particle in one system as it undergoes a binary collision and on the corresponding particle in the other system as it undergoes the corresponding collision. The first quantities calculated are the single-particle position and velocity differences between the two systems after the collision in terms of these differences before the collision. The final differences are then extended to give the values of the initial differences in the following collision. This procedure yields a set of difference equations for the single-particle position

and velocity differences. These equations are solved approximately by means of an averaging process. The resulting average solutions for the single-particle differences are used to produce averaged expressions for the N-particle distances D_q and D_p defined by Eqs. (11) and (12). Finally, an expression for the average exponentiation rates is obtained from the N-particle distances.

Assumptions

We expect collisions due to the hard core of the potential of Eq. (8) to be the dominant interaction among the particles since the attractive part of the potential is very weak and has a finite range. Moreover, the repulsive hard core of this potential is chosen[16] in particular because of its resemblance to a hard-sphere potential. Therefore, we elect to simplify our discussion by considering a hard-sphere gas. We confine our attention to gas systems whose particles move in only two spatial dimensions.

Definitions

Consider two macroscopically identical, N-particle, hard-sphere gas systems. Denote the Cartesian position and velocity vectors of the gas particles by $\vec{r}_1,\ldots,\vec{r}_N$ and $\vec{u}_1,\ldots,\vec{u}_N$ in the first system and by $\vec{r}_1',\ldots,\vec{r}_N'$ and $\vec{u}_1',\ldots,\vec{u}_N'$ in the second. For the kth particle of each system, define $\delta\vec{r}_k$ and $\delta\vec{u}_k$ to be the single-particle differences in position and velocity between the two systems, as given by

$$\delta\vec{r}_k = \vec{r}_k' - \vec{r}_k , \qquad (15a)$$

$$\delta\vec{u}_k = \vec{u}'_k - \vec{u}_k \ . \tag{15b}$$

We shall uniformly use a small δ, as in Eqs. (15), to denote the difference in a quantity between the two systems. Such differences are always assumed to be sufficiently small that second and higher-order terms in them may be neglected in the calculation. Because we work only to first order in δ-quantities, it is permissible and frequently expedient to treat δ as a differential operator applied to the unprimed quantities, and we do so several times in the course of the discussion.

The immediate objective of this calculation is to find the differences of Eqs. (15) as functions of time, for then D_q and D_p of Eqs. (11) and (12) can be computed from

$$D_q = \sqrt{\sum_{k=1}^{N} (\delta\vec{r}_k)^2} \ , \tag{16}$$

$$D_p = \sqrt{\sum_{k=1}^{N} (m\delta\vec{u}_k)^2} \ , \tag{17}$$

where m, the mass of a gas particle, is unity in the computer dimensions of Eqs. (8) and (9).

Before going into the detailed analysis, let us first define most of the quantities that will be needed and sketch an outline of the derivation. To avoid repetition, it will be our convention to define quantities only in the unprimed system. Such a definition will implicitly define both the equivalent quantity in the primed system and, as

in Eqs. (15), the difference in the quantity between the two systems. These implicitly-defined quantities will be denoted respectively by a prime and by the little-δ acting on the unprimed quantity, again as in Eqs. (15).

We examine the position and velocity differences of particle i as it undergoes a collision with particle j. In the following derivation, we temporarily use the special symbols $\vec{s}_i$, $\vec{s}_j$ and $\vec{v}_i$, $\vec{v}_j$ respectively for the positions and velocities of the particles immediately after the collision and reserve the symbols $\vec{r}_i$, $\vec{r}_j$ and $\vec{u}_i$, $\vec{u}_j$ for these quantities immediately before the collision. By immediately we here mean during some small (compared to the time between collisions) but non-zero time intervals after and before the collision. Later we shall evaluate the $\vec{r}$'s and $\vec{s}$'s at particular times (the $\vec{u}$'s and $\vec{v}$'s remain constant because of the free-particle dynamics), but until we do so, it should be kept in mind that these specially-defined position vectors are functions of time. When we arrive at the resulting difference equations, we shall return to the more general notation of Eqs. (15) through (17) in which $\vec{r}_k$ and $\vec{u}_k$ generically denote position and velocity.

For convenience we perform most of our calculation in the center-of-mass frame of the unprimed system; this frame is diagramed in Figure 2. Several center-of-mass quantities will be required, beginning with the initial and final relative velocities $\vec{u}$ and $\vec{v}$ defined by

$$\vec{u} = \vec{u}_i - \vec{u}_j , \tag{18}$$

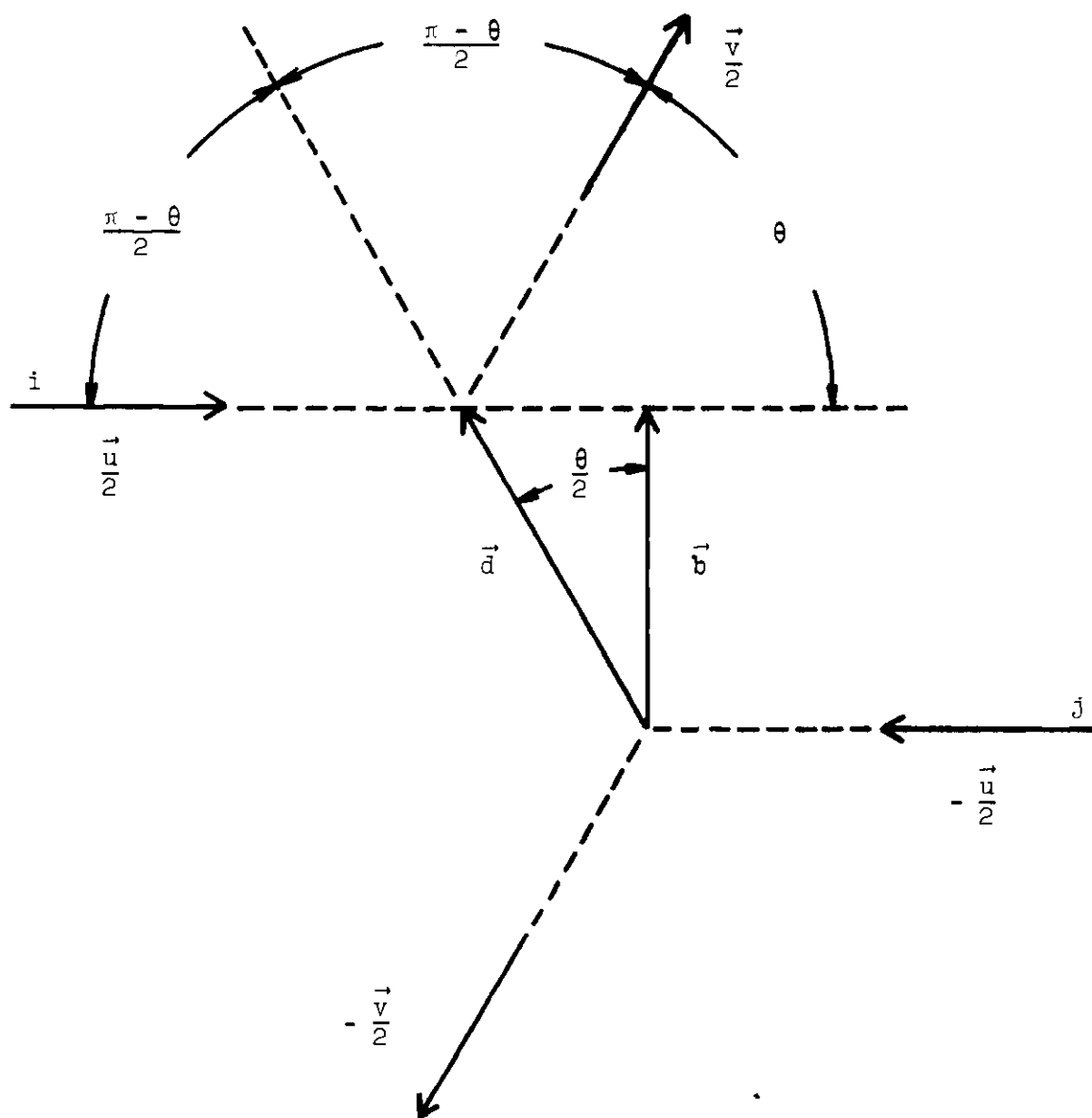$$\vec{v} = \vec{v}_i - \vec{v}_j . \tag{19}$$

Figure 2. Center-of-Mass Frame.

The initial and final velocities of particle i in the center-of-mass frame are $\vec{u}/2$ and $\vec{v}/2$, while those of particle j are $-\vec{u}/2$ and $-\vec{v}/2$. Similarly, we define the relative position vectors $\vec{r}$ and $\vec{s}$ to be given by

$$\vec{r}(t) = \vec{r}_i(t) - \vec{r}_j(t) , \tag{20}$$

$$\vec{s}(t) = \vec{s}_i(t) - \vec{s}_j(t) , \tag{21}$$

which are the vectors drawn from particle j to particle i before and after the collision, respectively.

Now define the scattering angle θ as the angle measured from $\vec{u}$ to $\vec{v}$. Because energy is conserved in the collision, we have

$$\vec{v} = R(\theta)\vec{u} , \tag{22}$$

where $R(\theta)$ is the rotation operator given by

$$R(\theta) = \begin{bmatrix} \cos\theta & -\sin\theta \\ \sin\theta & \cos\theta \end{bmatrix} . \tag{23}$$

Finally, let the impact parameter b be the projection of $\vec{r}$ perpendicular to $\vec{u}$ (this slightly unusual definition of the impact parameter will be discussed later). For hard spheres, the scattering angle θ is a function of b alone; we represent this fact by writing

$$\theta = \theta(b) . \tag{24}$$

Briefly, the derivation will go as follows. The initial

differences $\delta\vec{r}_i$, $\delta\vec{r}_j$, $\delta\vec{u}_i$, and $\delta\vec{u}_j$ in the lab frame cause conditions in the center-of-mass frame to differ between the two systems by $\delta\vec{r}$ and $\delta\vec{u}$ (which are implicitly defined by Eqs. (18) and (20) according to our convention). This produces a difference δb in the impact parameter which, in turn, generates a difference $\delta\theta$ between the scattering angles of the two systems. The difference $\delta\vec{v}$ in the final velocity $\vec{v}$ is then obtained with the help of Eq. (22).

After finding the velocity difference, we next compute from $\delta\vec{r}$ the difference $\delta\vec{s}$ in position after the collision by introducing a certain reflection operator. The final center-of-mass differences $\delta\vec{v}$ and $\delta\vec{s}$ are then transformed back to the lab frame to give the final differences $\delta\vec{v}_i$ and $\delta\vec{s}_i$ for particle i. Finally, we use free-particle dynamics to get the initial position and velocity differences for the next successive collision of particle i. Thus, we obtain a set of equations for the initial differences of a collision in terms of the initial differences of the preceding one. We then solve these equations approximately and find an expression to be compared with the experimentally observed exponenentiation rates.

Velocity Difference

We now begin the detailed calculations by finding first the final velocity difference $\delta\vec{v}$. In our notation, the magnitude of a vector will be indicated, unless otherwise specified, by omitting the vector symbol ($\rightarrow$), and a unit vector will always be denoted by a hat ($\wedge$), as in Eq. (25) below.

It will be expedient to introduce the orthogonal unit vectors $\hat{u}$

and $\hat{b}$ defined by

$$\hat{u} = \vec{u}/u \; , \tag{25}$$

$$\hat{b} = R\left(\frac{\pi}{2}\right)\hat{u} \; , \tag{26}$$

where R is the rotation operator of Eq. (23). The impact parameter b may then be written as

$$b = \vec{r}\cdot\hat{b} \; , \tag{27}$$

and we define the impact vector $\vec{b}$ by

$$\vec{b} = b\hat{b} \; . \tag{28}$$

It is always possible to pick the direction of positive rotation in such a way as to make b non-negative according to Eq. (27), but we do not choose to do so. Instead, we take the direction of positive rotation to be given, allow negative values for b, and let the scattering angle θ range from zero to 2π. This procedure allows the same positive rotation direction to be maintained throughout a sequence of collisions. This will be important later when we solve the difference equations. Since b can be negative, it is not the magnitude of the impact vector $\vec{b}$ of Eq. (28) but rather is the quantity defined by Eq. (27).

Although we shall not need it immediately, we complete the definitions for this section here by defining the vector $\vec{d}$, as shown in Figure 2, to be the common value of $\vec{r}$ and $\vec{s}$ at the instant of collision, that is,

$$\vec{d} = \vec{r}(t_c) = \vec{s}(t_c) \; , \tag{29}$$

where t_c is the time of the collision. The magnitude d of the vector $\vec{d}$ is just the diameter of the hard spheres of the gas.

We now find the difference δb in the impact parameter of Eq. (27). This may be done by finding $\delta\vec{b}$ (defined implicitly by Eq. (27)) and then using

$$\delta b = \hat{b} \cdot \delta\vec{b} . \tag{30}$$

It is to be emphasized that δb is the difference $(b'-b)$ and not the magnitude of $\delta\vec{b}$, according to our convention.

The truth of Eq. (30) can be seen easily by dotting $\hat{b}$ with Eq. (27) to give

$$b = \vec{b} \cdot \hat{b} \tag{31}$$

and applying the δ operator to Eq. (31) to yield

$$\delta b = \hat{b} \cdot \delta\vec{b} + \vec{b} \cdot \delta\hat{b} . \tag{32}$$

Now, since $\hat{b}$ has constant length, $\delta\hat{b}$ is orthogonal to $\vec{b}$, the last term of Eq. (32) vanishes, and Eq. (30) is established.

As $\vec{b}$ is the vector projection of $\vec{r}$ perpendicular to $\vec{u}$ (cf. Eqs. (27) and (28)), we have

$$\vec{b} = \vec{r} - \frac{(\vec{r}\cdot\vec{u})}{u^2} \vec{u} . \tag{33}$$

Application of the δ operator to Eq. (33) gives

$$\delta\vec{b} = \delta\vec{r} - \frac{(\vec{r}\cdot\vec{u})}{u^2} \delta\vec{u} - \vec{u}\, \delta\left(\frac{\vec{r}\cdot\vec{u}}{u^2}\right) . \tag{34}$$

Hence, from Eqs. (30) and (34), we obtain

$$\delta b = \hat{b} \cdot \delta \vec{r} - \frac{(\vec{r} \cdot \vec{u})}{u^2} \hat{b} \cdot \delta \vec{u} . \tag{35}$$

We next want to simplify Eq. (35) by evaluating $\vec{r}$ and $\delta \vec{r}$, which are functions of time, at the collision time t_c. Here we must be especially careful because $\delta \vec{r}$ has not been defined at the time t_c if the collision time t_c' in the primed frame happens to be earlier than t_c. To clarify this, we compute $\delta \vec{r}$ explicitly: we write

$$\vec{r}(t) = \vec{d} + (t - t_c)\vec{u}, \quad t \lesseqgtr t_c , \tag{36}$$

which follows from Eq. (29) and free-particle dynamics. The equivalent relation in the primed frame, valid for t earlier than t_c', is

$$\vec{r}'(t) = \vec{d}' + (t - t_c')\vec{u}', \quad t \lesseqgtr t_c' . \tag{37}$$

On subtracting Eq. (36) from Eq. (37), we have

$$\delta \vec{r}(t) = \delta \vec{d} + (t - t_c)\delta \vec{u} - \vec{u} \, \delta t_c , \tag{38}$$

but Eq. (38) is valid only for times up to the earlier of t_c and t_c'. We shall call the earlier of t_c and t_c' the beginning of the collision process, and the later, the end. At the beginning of the collision process, Eq. (38) becomes, to first order,

$$\delta \vec{r} = \delta \vec{d} - \vec{u} \, \delta t_c . \tag{39}$$

In obtaining Eq. (39), we have evaluated Eq. (38) at the earlier of t_c

and t'_c and then dropped the middle term which is either zero or at most of second order. The $\delta\vec{r}$ of Eq. (39) is well defined and is the particular value we want to consider as the initial position difference for the collision under investigation.

Hereafter, we shall use the symbol $\delta\vec{r}$ exclusively to mean the quantity given in (essentially defined by) Eq. (39), although it will not be convenient to substitute for $\delta\vec{r}$ from this equation because experimentally $\delta\vec{r}$ is known while $\delta\vec{d}$ and δt_c are not.

Eq. (35) for δb is valid for any time up to the beginning of the collision process. We therefore evaluate this equation at the beginning of the collision process and substitute for $\vec{r}$ from Eq. (36) then to yield, to first order,

$$\delta b = \hat{b}\cdot\delta\vec{r} - \frac{(\vec{d}\cdot\vec{u})}{u^2}\, \hat{b}\cdot\delta\vec{u} \quad . \tag{40}$$

From the conservation of linear and angular momentum, it can be shown that the line of $\vec{d}$ bisects the supplement $(\pi - \theta)$ of the scattering angle θ as shown in Figure 2. Thus, the angle from $\hat{b}$ to $\vec{d}$ is $\theta/2$, and we write

$$\vec{d} = d\, R\!\left(\frac{\theta}{2}\right)\, \hat{b} \quad . \tag{41}$$

Hence, with the help of Eq. (26), we have

$$\vec{d}\cdot\vec{u} = -\, u\, d\, \sin\frac{\theta}{2} \quad . \tag{42}$$

Therefore, Eq. (40) becomes

$$\delta b = \hat{b} \cdot \vec{\delta r} + \frac{d}{u} \sin \frac{\theta}{2} \, \hat{b} \cdot \vec{\delta u} \, , \tag{43}$$

which completes the determination of δb.

Our next step is to find $\delta \theta$, the difference in the scattering angle. From Eq. (24) we obtain

$$\delta \theta = \frac{\partial \theta}{\partial b} \, \delta b \, , \tag{44}$$

where we use the partial derivative notation to keep in mind that θ in general, as opposed to the hard-sphere case considered here, depends on u as well as b. Now evaluate Eq. (27) at the time t_c, with the help of Eqs. (29) and (41), to get

$$b = d \cos \frac{\theta}{2} \, . \tag{45}$$

Hence, we have

$$\frac{\partial \theta}{\partial b} = \frac{-2}{d \sin \frac{\theta}{2}} \, . \tag{46}$$

Eqs. (43) and (46) may now be substituted into Eq. (44) to yield

$$\delta \theta = - \frac{2 \hat{b} \cdot \vec{\delta r}}{d \sin \frac{\theta}{2}} - \frac{2 \hat{b} \cdot \vec{\delta u}}{u} \, . \tag{47}$$

It remains to compute the final velocity difference $\vec{\delta v}$ from $\delta \theta$ of Eq. (47). Eq. (22), written explicitly for the primed system, is

$$\vec{v}' = R(\theta + \delta \theta) \vec{u}' \, . \tag{48}$$

Using Eq. (23), the rotation in Eq. (48) can be shown to be given by

$$R(\theta + \delta\theta) = R(\theta) + \delta\theta\, R(\theta)R\!\left(\frac{\pi}{2}\right) . \tag{49}$$

We put Eq. (49) into (48), and use Eq. (22) and the definition

$$\vec{u}' = \vec{u} + \delta\vec{u} , \tag{50}$$

to obtain, after some rearrangement,

$$\delta\vec{v} = R(\theta)(\delta\vec{u} + u\hat{b}\delta\theta) . \tag{51}$$

By substitution of Eq. (47) into (51), we find $\delta\vec{v}$ to be given by

$$\delta\vec{v} = R(\theta)\left[\delta\vec{u} - 2\hat{b}(\hat{b}\cdot\delta\vec{u}) - \frac{2u\hat{b}(\hat{b}\cdot\delta\vec{r})}{d\,\sin\frac{\theta}{2}} \right] , \tag{52}$$

which was the objective of this section.

Position Difference

The final position difference $\delta\vec{s}$ will now be calculated. As with $\delta\vec{r}$, we must be careful to state at what time $\delta\vec{s}$ is to be found, for it has not been defined at times before the later of t_c and t'_c. In the terminology of the preceding section, $\delta\vec{s}$ is not defined before the end of the collision process.

With the use of Eq. (29), we write, in analogy with Eq. (36),

$$\vec{s} = \vec{d} + (t - t_c)\vec{v} , \quad t \geqq t_c . \tag{53}$$

Eq. (53), in analogy with Eq. (38), leads to

$$\delta\vec{s} = \delta\vec{d} + (t - t_c)\delta\vec{v} - \vec{v}\delta t_c , \qquad (54)$$

valid at and after the end of the collision process. No matter which
of t_c or t_c' is later, however, to first order $\delta\vec{s}$ at the end of the col-
lision process is given by

$$\delta\vec{s} = \delta\vec{d} - \vec{v}\delta t_c , \qquad (55)$$

which is to be compared with Eq. (39) for $\delta\vec{r}$ at the beginning of the
collision process. After this, by $\delta\vec{s}$ we shall always mean the particu-
lar one given by Eq. (55), just as by $\delta\vec{r}$ we mean the one of Eq. (39).

Now let P be the operator that reflects a vector through the $\hat{u}$
axis. As any vector $\vec{a}$ may be written in the form

$$\vec{a} = a\,R(\alpha)\hat{u} , \qquad (56)$$

for some angle α, the result of P acting on such an $\vec{a}$ may be written

$$P\vec{a} = a\,R(-\alpha)\hat{u} . \qquad (57)$$

It will now be shown that $\delta\vec{r}$ and $\delta\vec{s}$ are related by

$$\delta\vec{s} = R(\theta)P\,\delta\vec{r} . \qquad (58)$$

We must have $\delta\vec{d}$ perpendicular to $\vec{d}$ because $\vec{d}$ has constant length; thus,
with the help of Eq. (41), we may write $\delta\vec{d}$ as

$$\delta\vec{d} = \xi\left|\delta\vec{d}\right|R\left(\frac{\theta}{2}\right)\hat{u} , \qquad (59)$$

where ξ is ± 1. Hence, from Eqs. (57) and (59), we obtain

$$P \ \delta\vec{d} = \xi \left| \delta\vec{d} \right| R\left(- \frac{\theta}{2}\right) \hat{u} \ . \tag{60}$$

Therefore, by means of Eq. (59), $R(\theta)$ applied to Eq. (60) gives

$$R(\theta) \ P \ \delta\vec{d} = \delta\vec{d} \ . \tag{61}$$

Further, we note from Eqs. (57) and (22) that

$$R(\theta) \ P \ \vec{u} = \vec{v} \ . \tag{62}$$

Let us now operate on $\delta\vec{r}$ with the composite operator $R(\theta)P$. In the process we substitute from Eqs. (39) and (55) and use Eqs. (61) and (62) to obtain

$$R(\theta) \ P \ \delta\vec{r} = R(\theta) \ P \ \left(\delta\vec{d} - \vec{u} \ \delta t_c \right) \tag{63}$$

$$= R(\theta) \ P \ \delta\vec{d} - \vec{v} \ \delta t_c$$

$$= \delta\vec{d} + \delta\vec{s} - \delta\vec{d} \ ;$$

so Eq. (58) is proved.

Difference Equations

At this point we have found, in Eqs. (52) and (58), expressions for $\delta\vec{v}$ and $\delta\vec{s}$ at the end of the collision process in terms of center-of-mass quantities. Before going on to write the corresponding equations in the lab frame, let us rewrite Eq. (52) according to the following consideration.

From Eq. (56) it can be seen that

$$P \ \hat{u} = \hat{u} \ , \tag{64}$$

$$P \hat{b} = - \hat{b} . \tag{65}$$

But, since any vector $\vec{a}$ may be written as

$$\vec{a} = (\vec{a} \cdot \hat{u})\hat{u} + (\vec{a} \cdot \hat{b})\hat{b} , \tag{66}$$

we have, from Eqs. (64) through (66), the identity

$$P \vec{a} = (\vec{a} \cdot \hat{u})\hat{u} - (\vec{a} \cdot \hat{b})\hat{b} \tag{67}$$

$$= \vec{a} - 2(\vec{a} \cdot \hat{b})\hat{b} .$$

Thus, with Eq. (67), we can rewrite Eq. (52) as

$$\delta\vec{v} = R(\theta)P \ \delta\vec{u} - \frac{2uR(\theta)\hat{b}}{d \sin \frac{\theta}{2}} (\hat{b} \cdot \delta\vec{r}) , \tag{68}$$

which is to be compared with Eq. (58) for $\delta\vec{s}$.

Now let us transform $\delta\vec{v}$ and $\delta\vec{s}$ of Eqs. (68) and (58) to the lab frame. The lab frame final velocity $\vec{v}_i$ and position $\vec{s}_i$ are given by

$$\vec{v}_i = \frac{\vec{u}_i + \vec{u}_j}{2} + \frac{\vec{v}}{2} , \tag{69}$$

$$\vec{s}_i = \frac{\vec{r}_i + \vec{r}_j}{2} + \frac{\vec{s}}{2} , \tag{70}$$

where $\vec{u}_i$, $\vec{u}_j$, $\vec{r}_i$, and $\vec{r}_j$ are taken at the beginning of the collision process, and $\vec{v}_i$, $\vec{v}$, $\vec{s}_i$, and $\vec{s}$ at the end. Eq. (70) is valid only to zeroth order, as we have dropped a term on the order of $(\vec{u}_i + \vec{u}_j)\delta t_c$. However, the equations for the differences $\delta\vec{v}_i$ and $\delta\vec{s}_i$ are valid to first order; we write them explicitly:

$$\delta \vec{v}_i = \frac{\delta \vec{u}_i + \delta \vec{u}_j}{2} + \frac{\delta \vec{v}}{2} \ , \tag{71}$$

$$\delta \vec{s}_i = \frac{\delta \vec{r}_i + \delta \vec{r}_j}{2} + \frac{\delta \vec{s}}{2} \ . \tag{72}$$

In order to proceed we must consider successive collisions of a particle. For any particle k, let the single-particle collision index $n_k(t)$ be defined as the total number of collisions undergone by particle k from the initial time t = 0 through the time t. Let $t_{k,n}$ be the time of the beginning of the nth collision of particle k, where "beginning" is used in the special sense that has been defined. We shall usually omit the explicit time dependence of the collision index and write simply n_k, or just n when the particle meant is clear from the context.

We now revert to our earlier notation in which the position and velocity of any particle k at time t are denoted by $\vec{r}_k(t)$ and $\vec{u}_k(t)$. We immediately introduce the following special notation for $\vec{u}_k$ and $\vec{r}_k$ at the beginning of the nth collision of particle k: define $\vec{u}_{k,n}$ and $\vec{r}_{k,n}$ by

$$\vec{u}_{k,n} = \vec{u}_k(t_{k,n}) \ , \tag{73}$$

$$\vec{r}_{k,n} = \vec{r}_k(t_{k,n}) \ , \tag{74}$$

where n is understood to mean the collision index n_k for particle k.

Suppose that the particular collision we have been examining is number n_i for particle i and number n_j for particle j. The old $\delta \vec{r}_i$ and $\delta \vec{r}_j$ of Eq. (72) go over into the new notation of Eq. (74) according to

$$\delta \vec{r}_i \rightarrow \delta \vec{r}_{i,n} , \tag{75}$$

$$\delta \vec{r}_j \rightarrow \delta \vec{r}_{j,n} . \tag{76}$$

A similar change of $\delta \vec{u}_i$ and $\delta \vec{u}_j$ of Eq. (71) into the notation of Eq. (73) is given by

$$\delta \vec{u}_i \rightarrow \delta \vec{u}_{i,n} , \tag{77}$$

$$\delta \vec{u}_j \rightarrow \delta \vec{u}_{j,n} . \tag{78}$$

It is to be understood that the n of Eqs. (75) and (77) is n_i, whereas the n of Eqs. (76) and (78) is n_j.

We want to write a set of equations for the beginning conditions of successive collisions, but we have obtained end conditions in Eqs. (71) and (72). The beginning conditions of the next (i.e., n + 1st) collision are easily found, however. The velocities do not change between collisions, so we have

$$\delta \vec{u}_{i,n+1} = \delta \vec{v}_i , \tag{79}$$

where $\delta \vec{v}_i$ is from Eq. (71). The change in position difference is found from free-particle dynamics to be

$$\delta \vec{r}_{i,n+1} = \delta \vec{s}_i + \tau_{i,n+1} \, \delta \vec{u}_{i,n+1} , \tag{80}$$

where $\delta \vec{s}_i$ is from Eq. (72), and where $\tau_{i,n+1}$ is defined to be the time interval between the collisions n and n+1 of particle i according to

$$\tau_{i,n+1} = t_{i,n+1} - t_{i,n} \; . \tag{81}$$

Thus, from Eqs. (79) and (80), by using Eqs. (71) and (72), by substituting from Eqs. (68) and (58), and by employing the definitions of $\delta\vec{u}$ and $\delta\vec{r}$ implicit in Eqs. (18) and (20), we obtain

$$\delta\vec{u}_{i,n+1} = \frac{\delta\vec{u}_{i,n} + \delta\vec{u}_{j,n}}{2} + R(\theta_n)P_n \left(\frac{\delta\vec{u}_{i,n} - \delta\vec{u}_{j,n}}{2} \right) \tag{82}$$

$$- \frac{2u_n R(\theta_n)\hat{b}_n}{d \sin\frac{\theta_n}{2}} \hat{b}_n \cdot \left(\frac{\delta\vec{r}_{i,n} - \delta\vec{r}_{j,n}}{2} \right) \quad ,$$

$$\delta\vec{r}_{i,n+1} = \frac{\delta\vec{r}_{i,n} + \delta\vec{r}_{j,n}}{2} + R(\theta_n)P_n \left(\frac{\delta\vec{r}_{i,n} - \delta\vec{r}_{j,n}}{2} \right) \tag{83}$$

$$+ \tau_{i,n+1}\delta\vec{u}_{i,n+1} \quad ,$$

where the n subscripts on the center-of-mass quantities $(u_n,\ \theta_n,\ P_n,$ etc.) refer to those quantities in the nth collision of particle i.

In Eqs. (82) and (83), we intend that the particle index i range over all the particles to produce a set of 2N simultaneous vector difference equations, the solution of which would give the $\delta\vec{r}_i$ and $\delta\vec{u}_i$ for all N particles as functions of the N collision indices n_i. As they stand, these equations are incomplete, because there is no specification of the center-of-mass quantities $(u_n,$ etc.) nor of the times $\tau_{i,n+1}$ between collisions. To specify these quantities, we should have to solve the equations of motion (Eqs. (2) and (3)) for the gas system. As the exact solution of neither Eqs. (2) and (3) nor Eqs. (82) and (83) is possible, we attempt a statistical solution of them.

Solutions

Using a statistical method, we next solve Eqs. (82) and (83)
approximately. The statistical assumptions introduced in the solutions
preclude any theoretical proof of the stochastic character of our model
by these methods. The hard-sphere gas has been shown by Sinai[2,12] to
be essentially a C-system; in particular, the two-particle, two-
dimensional, hard-sphere gas we next consider is of this class.[2] There-
fore, one would expect statistical methods to be valid. Our purpose in
what follows is not a proof of stochasticity but rather a computation of
formulas to be compared with experiment. We rely on Sinai's theorems
to justify many assumptions that would not be allowed in a rigorous dis-
cussion.

Two-Particle Solution

Before finding an approximate, general solution of Eqs. (82) and
(83), we find statistical solutions of these equations for a two-particle
system that has periodic boundary conditions as in our computer experi-
ments. This case is considered first because it is more nearly rigorous
than the general solution we shall present but nevertheless contains
most of the same features.

We initially take the total linear momentum to be zero in both
the primed and unprimed systems and translate one system, if necessary,
so the two centers of mass coincide. The lab and center-of-mass frames
are then identical for both systems and will remain so as the systems
evolve because the total linear momentum is conserved. Thus, in the
notation of Eqs. (73) and (74), we have for all n that

$$\vec{u}_{i,n} + \vec{u}_{j,n} = 0 \ , \tag{84}$$

$$\vec{r}_{i,n} + \vec{r}_{j,n} = \text{constant} \ , \tag{85}$$

where i and j represent the two particles. The corresponding position and velocity differences between the two systems are therefore related by

$$\delta\vec{u}_{i,n} = - \ \delta\vec{u}_{j,n} \ , \tag{86}$$

$$\delta\vec{r}_{i,n} = - \ \delta\vec{r}_{j,n} \ , \tag{87}$$

for every n. The n of these last four equations is clearly the same for both particles, as the two must always collide with each other.

In order to satisfy the C-system criteria, as stated in connection with Eqs. (5) and (6), we must select the differences of Eqs. (86) and (87) to be both on the energy surface of the unprimed system and normal to the unprimed trajectory there. These restrictions could be accomplished by requiring that the initial differences $\delta\vec{u}_{i,o}$ and $\delta\vec{r}_{i,o}$ satisfy

$$\delta\vec{u}_{i,o} \cdot \vec{u}_{i,o} = 0 \ , \tag{88}$$

$$\delta\vec{r}_{i,o} \cdot \vec{u}_{i,o} = 0 \ , \tag{89}$$

in addition to Eqs. (86) and (87). For the present, however, we omit applying the restrictions of Eqs. (88) and (89) in order to bring out certain features of the solutions which have a bearing on our computer experiments, as will be discussed.

Substitution of Eqs. (86) and (87) into Eqs. (82) and (83) yields

$$\vec{\delta u}_{i,n+1} = R(\theta_n)P_n\vec{\delta u}_{i,n} - \frac{2u\,R(\theta_n)\hat{b}_n}{d\,\sin\frac{\theta_n}{2}}\,\hat{b}_n\cdot\vec{\delta r}_{i,n} \,, \tag{90}$$

$$\vec{\delta r}_{i,n+1} = R(\theta_n)P_n\vec{\delta r}_{i,n} + \tau_{n+1}\,\delta u_{i,n+1} \,, \tag{91}$$

where we have dropped the n-subscript from u_n of Eq. (82) because u is a constant of the motion in Eq. (90) and the i-subscript from $\tau_{i,n+1}$ because τ_{n+1} is the same for both particles. Since the lab frame is the center-of-mass frame, we have

$$\hat{u}_{n+1} = R(\theta_n)\,\hat{u}_n \,, \tag{92}$$

and hence, from Eq. (26), we also have

$$\hat{b}_{n+1} = R(\theta_n)\,\hat{b}_n \,. \tag{93}$$

It would be necessary to insert the possibility of a reflection as well as a rotation into Eq. (93) had we not allowed negative values of the impact parameter b of Eq. (27). The negative values were originally allowed to avoid this reflection.

With the help of Eqs. (92), (93), and (67), we next resolve the difference vectors of Eqs. (90) and (91) into components along the center of mass axes $\hat{u}_n$, $\hat{b}_n$, $\hat{u}_{n+1}$, and $\hat{b}_{n+1}$ as appropriate to the nth or n+1st collisions. In so doing, for notational convenience, we make the following definitions:

$$\delta x_n = \hat{u}_n\cdot\vec{\delta r}_{i,n} \,, \tag{94}$$

$$\delta y_n = \hat{b}_n \cdot \delta \vec{r}_{i,n} \; , \tag{95}$$

$$\delta z_n = \hat{u}_n \cdot \delta \vec{u}_{i,n} \; , \tag{96}$$

$$\delta w_n = \hat{b}_n \cdot \delta \vec{u}_{i,n} \; , \tag{97}$$

which are to hold for any n. For the $\hat{u}$ components we obtain, with the help of Eq. (92),

$$\delta z_{n+1} = \delta z_n \; , \tag{98}$$

$$\delta x_{n+1} = \delta x_n + \tau_{n+1} \delta z_{n+1} \; , \tag{99}$$

while for the $\hat{b}$ components we get, with the help of Eq. (93),

$$\delta w_{n+1} = -\delta w_n - \frac{2u}{d \sin \frac{\theta_n}{2}} \delta y_n \; , \tag{100}$$

$$\delta y_{n+1} = -\delta y_n + \tau_{n+1} \, \delta w_{n+1} \; . \tag{101}$$

Eqs. (98) and (99) have the immediate solutions

$$\delta z_n = \delta z_o \; , \tag{102}$$

$$\delta x_n = \delta x_o + t_n \delta z_o \; , \tag{103}$$

where t_n is the time of the nth collision (relative to $t_o=0$), and the initial conditions δz_o and δx_o are given.

We now apply the restrictions of Eqs. (88) and (89), which, in view of Eqs. (94) and (96), give

$$\delta z_o = 0 , \qquad (104)$$

$$\delta x_o = 0 . \qquad (105)$$

Thus, Eqs. (102) and (103) become

$$\delta z_n = 0 , \qquad (106)$$

$$\delta x_n = 0 , \qquad (107)$$

for all n.

From Eqs. (102) and (103) we can see the features referred to earlier that are pertinent to the computer experiments. In the experiments, an approximate algorithm was used to satisfy the appropriately generalized equivalents of Eqs. (88) and (89). Sometimes there resulted a small component of the initial differences normal to the energy surface or parallel to the trajectory, in analogy with δz_o and δx_o. One can argue in considerable detail, however, that the analog of Eqs. (102) and (103) should hold for a system of any number of particles, provided that the particles are sufficiently similar to hard spheres, as we have assumed ours to be. Therefore, these initial differences contribute at most a linear time dependence to D_q and D_p of Eqs. (11) and (12). This linear dependence is quickly dominated by the experimentally observed exponentiation.

We return now to the solutions for δw and δy. Eqs. (100) and (101) can be separated into two second-order equations, each involving only one of δw and δy. The separation gives

$$\delta w_{n+2} + \left[1 + \frac{2u\tau_{n+1}}{d \, \sin \frac{\theta_{n+1}}{2}} + \frac{\sin \frac{\theta_n}{2}}{\sin \frac{\theta_{n+1}}{2}} \right] \delta w_{n+1} + \frac{\sin \frac{\theta_n}{2}}{\sin \frac{\theta_{n+1}}{2}} \, \delta w_n = 0 \ , \qquad (108)$$

$$\delta y_{n+2} + \left[1 + \frac{2u\tau_{n+2}}{d \, \sin \frac{\theta_{n+1}}{2}} + \frac{\tau_{n+2}}{\tau_{n+1}} \right] \delta y_{n+1} + \frac{\tau_{n+2}}{\tau_{n+1}} \, \delta y_n = 0 \ . \qquad (109)$$

To solve Eqs. (108) and (109), we assume that each collision n is an independent event in which θ_n and τ_n are selected independently according to appropriate probability distributions. (When we evaluate the averages in Appendix B, we use a Maxwell, i.e., canonical, velocity distribution.) In addition, we consider an ensemble of unprimed systems that extends over all possible microscopic states consistent with the macroscopic conditions. From it we obtain an associated, primed ensemble by requiring the initial differences δw_0, δy_0, δz_0, and δx_0 to be the same in every case. Our objective is to solve for the ensemble averages of δw_n and δy_n.

In Appendix A, it is shown that the approximations

$$\left\langle \frac{1}{\sin \frac{\theta_n}{2}} \right\rangle \approx \frac{1}{\left\langle \sin \frac{\theta_n}{2} \right\rangle} \ , \qquad (110)$$

$$\left\langle \frac{1}{\tau_n} \right\rangle \approx \frac{1}{\langle \tau_n \rangle} \ , \qquad (111)$$

where the angular brackets indicate an ensemble average, allow Eqs. (108) and (109) to be written for the ensemble everages of δw_n and δy_n by averaging the coefficients.

The procedure of averaging the coefficients in Eqs. (108) and (109) gives

$$\delta w_{n+2} + 2\left(1 + \frac{mu\tau}{2d}\right)\delta w_{n+1} + \delta w_n = 0 , \tag{112}$$

$$\delta y_{n+2} + 2\left(1 + \frac{mu\tau}{2d}\right)\delta y_{n+1} + \delta y_n = 0 , \tag{113}$$

where all quantities are ensemble averages. The average of $\sin \frac{\theta_n}{2}$ is taken from Eq. (B17) of Appendix B. For the initial conditions, a similar average of Eqs. (100) and (101) is needed, which gives

$$\delta w_1 = - \delta w_o - \frac{mu}{d} \delta y_o , \tag{114}$$

$$\delta y_1 = - \delta y_o + \tau \, \delta w_1 , \tag{115}$$

where again all quantities are ensemble averages with the exception of δw_o and δy_o which are the given initial conditions.

With the initial conditions of Eqs. (114) and (115), the solutions of Eqs. (112) and (113) can be shown to be

$$\delta w_n = \frac{(-1)^n}{2 \sinh \gamma} \left\{ \left[(1 - e^{-\gamma})\delta w_o + \frac{mu}{d} \delta y_o\right] e^{\gamma n} \right. \tag{116}$$

$$\left. + \left[(e^\gamma - 1)\delta w_o - \frac{mu}{d} \delta y_o\right] e^{-\gamma n} \right\} ,$$

$$\delta y_n = \frac{(-1)^n}{2 \sinh \gamma} \left\{ \left[(e^\gamma - 1)\delta y_o + \tau \delta w_o\right] e^{\gamma n} \right. \tag{117}$$

$$\left. + \left[(1 - e^{-\gamma})\delta y_o - \tau \delta w_o\right] e^{-\gamma n} \right\} ,$$

where γ is here given by

$$\gamma = \cosh^{-1}\left(1 + \frac{m_u \tau}{2d}\right) \quad . \tag{118}$$

From Eqs. (94) through (97), (106), and (107), we have

$$\left|\delta\vec{u}_n\right| = \left|\delta w_n\right| \quad , \tag{119}$$

$$\left|\delta\vec{r}_n\right| = \left|\delta y_n\right| \quad . \tag{120}$$

Suppose we choose δw_o and δy_o to be related by

$$(e^\gamma - 1)\delta w_o = \frac{m_u}{d}\, \delta y_o \quad . \tag{121}$$

Then Eqs. (116), (119), and (111) combine to give

$$\left|\delta\vec{u}_n\right| = \left|\delta\vec{u}_o\right|e^{\gamma n} \quad , \tag{122}$$

and, with the additional help of Eq. (118), Eqs. (117), (120), and (121) give

$$\left|\delta\vec{r}_n\right| = \left|\delta\vec{r}_o\right|e^{\gamma n} \quad . \tag{123}$$

Eqs. (122) and (123) are to be compared with Eqs. (5).

If, instead of Eq. (121), we choose δw_o and δy_o to be related by

$$(e^\gamma - 1)\delta w_o = -\frac{m_u}{d}\, \delta y_o \quad , \tag{124}$$

then we similarly obtain

$$\left|\delta\vec{u}_n\right| = \left|\delta\vec{u}_o\right|e^{-\gamma n} \quad , \tag{125}$$

$$|\delta\vec{r}_n| = |\delta\vec{r}_o|e^{-\gamma n} , \qquad (126)$$

which are to be compared with Eqs. (6).

Thus, the choice of Eq. (121) determines the dilating space, and that of Eq. (124) determines the contracting space. Furthermore, γ of Eq. (118) is the ensemble average of the trajectory exponentiation rate (with respect to collision index n) for both position and velocity.

General Solution

An approximate, general solution of Eqs. (82) and (83) will now be found for a system of N particles. The problem will be approached in two parts: 1) find the overall effect of the sequence in which collisions occur and 2) find the quantitative effect of individual collisions. Once the first part is accomplished, the second becomes a straightforward generalization of the two-particle case. The difficulty is that there is no equivalent in the general case to Eqs. (86) and (87) of the two-particle case. This lack tends to destroy the causal relationship of a particle with its past. In the first part of the discussion we shall find a quantity that is causally related to its past and associate this quantity with the exponentiation of trajectories.

For brevity in the discussion, relational conditions are sometimes stated for vectors (e.g., the maximum $\delta\vec{u}$). These statements should be taken to apply to the magnitudes of the vectors. Also, the discussion will be carried through for the most part in terms of the $\delta\vec{u}$'s; it is to be understood that equivalent remarks hold for the $\delta\vec{r}$'s.

We make the following postulate, based on observation:

Postulate 1. The $\delta\vec{u}$'s and $\delta\vec{r}$'s of a system are distributed at any

instant over a wide magnitude range.

Empirically it was observed that typically a factor of 10^3 to 10^5 existed between the maximum and minimum $\delta\vec{u}$'s and $\delta\vec{r}$'s.

The experimental initial conditions put all of the $\delta\vec{u}$'s and $\delta\vec{r}$'s with the same magnitude, and it might be thought that at least one collision per particle would be required to establish the condition of Postulate 1. However, the crucial part of this postulate is that the maximum $\delta\vec{u}$ and $\delta\vec{r}$ in the system be much larger than most of the other $\delta\vec{u}$'s and $\delta\vec{r}$'s. This condition was observed experimentally to be established rather quickly (within 10 collisions or so of $t = 0$).

Two corollaries are obtained from Postulate 1:

Corollary 1a. In a large proportion of collisions, the initial $\delta\vec{u}$ and $\delta\vec{r}$ of one particle are much larger than the initial $\delta\vec{u}$ and $\delta\vec{r}$ of the other particle.

Corollary 1b. The maximum $\delta\vec{u}$ and $\delta\vec{r}$ of a system dominate the sums forming D_p and D_q of Eqs. (16) and (17).

Suppose particle i has the larger initial $\delta\vec{u}$ and $\delta\vec{r}$ in an i-j collision, as in Corollary 1a. Then we can neglect $\delta\vec{u}_{j,n}$ and $\delta\vec{r}_{j,n}$ in comparison with $\delta\vec{u}_{i,n}$ and $\delta\vec{r}_{i,n}$ in Eqs. (82) and (83) to obtain

$$\delta\vec{u}_{i,n+1} = \frac{\delta\vec{u}_{i,n}}{2} + R(\theta_n)P_n \frac{\delta\vec{u}_{i,n}}{2} - \frac{u_n R(\theta_n)\hat{b}_n}{d \sin \frac{\theta_n}{2}} (\hat{b}_n \cdot \delta\vec{r}_{i,n}) \, , \qquad (127a)$$

$$\delta\vec{r}_{i,n+1} = \frac{\delta\vec{r}_{i,n}}{2} + R(\theta_n)P_n \frac{\delta\vec{r}_{i,n}}{2} + \tau_{i,n+1} \delta\vec{u}_{i,n+1} \, , \qquad (127b)$$

$$\delta \vec{u}_{j,n+1} = \frac{\delta \vec{u}_{i,n}}{2} - R(\theta_n)P_n \frac{\delta \vec{u}_{i,n}}{2} + \frac{u_n \, R(\theta_n)\hat{b}_n}{d \, \sin \frac{\theta_n}{2}} \, (\hat{b}_n \cdot \delta \vec{r}_{i,n}) \, , \tag{127c}$$

$$\delta \vec{r}_{j,n+1} = \frac{\delta \vec{r}_{i,n}}{2} - R(\theta_n)P_n \frac{\delta \vec{r}_{i,n}}{2} + \tau_{j,n+1} \, \delta \vec{u}_{j,n+1} \, . \tag{127d}$$

If one substituted from Eqs. (127a) and (127c) on the right of Eqs. (127b) and (127d), then all four equations would have only $\delta \vec{u}_{i,n}$ and $\delta \vec{r}_{i,n}$ on the right. Thus, $\delta \vec{u}_{i,n+1}$ and $\delta \vec{r}_{i,n+1}$ are causally related to $\delta \vec{u}_{i,n}$ and $\delta \vec{r}_{i,n}$, but $\delta \vec{u}_{j,n+1}$ and $\delta \vec{r}_{j,n+1}$ are not causally related to $\delta \vec{u}_{j,n}$ and $\delta \vec{r}_{j,n}$. The future of particle j depends on the past of particle i. In fact, it can be shown from Eqs. (127) that on the average $\left| \delta \vec{u}_{j,n+1} \right|$ and $\left| \delta \vec{r}_{j,n+1} \right|$ are equal to $\left| \delta \vec{u}_{i,n+1} \right|$ and $\left| \delta \vec{r}_{i,n+1} \right|$. In this way, particle i communicates its past history to particle j insofar as the δ's are concerned; the past of particle j is irrelevant.

Hence, the $\delta \vec{u}_i$ for a particular particle i is not always causally related to its own past. Nevertheless, in certain sequences of collisions, it is possible to define a maximum $\delta \vec{u}$ that is causally related to its own past, although the particle with which this maximum $\delta \vec{u}$ is associated may change during the sequence. As an example of this, consider the sequence of collisions (1-2, 2-3, 3-4). Let us number these collisions for reference by the index n*: the 1-2 collision is number n^*_0, the 2-3 number $n^*_0 + 1$, etc. Note that n* is not associated with any single particle. We assume that a collision almost always acts to increase the $\delta \vec{u}$'s involved, because of the known[2,12] exponentiating character of this system and the argument in Chapter II about the dominance of the dilating space.

Suppose that initially $\delta\vec{u}_{1,n_0^*}$ is the maximum of the $\delta\vec{u}$'s. After the 1-2 collision $\delta\vec{u}_{1,n_0^*+1}$ and $\delta\vec{u}_{2,n_0^*+1}$ are the maxima, after the 2-3 collision $\delta\vec{u}_{2,n_0+2}$ and $\delta\vec{u}_{3,n_0+3}$ are the maxima, and after the 3-4 collision $\delta\vec{u}_{3,n_0^*+3}$ and $\delta\vec{u}_{4,n_0^*+4}$ are the maxima (similar comments apply to the $\delta\vec{r}$'s). Now observe that through Eqs. (127c) and (127d) we have $\delta\vec{u}_{2,n_0^*+1}$ (and $\delta\vec{r}_{2,n_0^*+1}$) causally related to $\delta\vec{u}_{1,n_0^*}$ (and $\delta\vec{r}_{1,n_0^*}$), $\delta\vec{u}_{3,n_0^*+2}$ causally related to $\delta\vec{u}_{2,n_0^*+1}$, and $\delta\vec{u}_{4,n_0^*+3}$ causally related to $\delta\vec{u}_{3,n_0^*+2}$. Thus $\delta\vec{u}_{n^*}$, defined by $(\delta\vec{u}_{n_0^*}, \delta\vec{u}_{n_0^*+1}, \delta\vec{u}_{n_0^*+2}, \delta\vec{u}_{n_0^*+3})$ being respectively equal to $(\delta\vec{u}_{1,n_0^*}, \delta\vec{u}_{2,n_0^*+1}, \delta\vec{u}_{3,n_0^*+2}, \delta\vec{u}_{4,n_0^*+3})$, is the maximum $\delta\vec{u}$ throughout the sequence and is causally related to its past.

It is not possible to define such a causally related $\delta\vec{u}$ throughout any sequence that includes a maximum (other than the first) generated by a collision outside the sequence. In our example, if $\delta\vec{u}_3$ had been larger than $\delta\vec{u}_2$ in the 2-3 collision, then the causal sequence would not have occurred. But there is one sequence (if it exists) for which it is always possible to define such a causal $\delta\vec{u}$, namely, the sequence in which a new maximum $\delta\vec{u}$ (and $\delta\vec{r}$) for the entire system is produced by each collision. In this sequence, the maximum $\delta\vec{u}$ at each collision is necessarily a result of the previous collision in the sequence. Furthermore, it is just this sequence which is of greatest interest, for by Corollary 1b the calculation of the maximum $\delta\vec{u}$ and $\delta\vec{r}$ is the calculation of D_p and D_q.

It is unlikely for a single sequence as just described to exist over a long period of time. However, we shall shortly make the approximation of replacing the collision parameters of Eqs. (82) and (83) by their averages, and in so doing we shall average over the directions of

the $\delta\vec{u}$'s and $\delta\vec{r}$'s. In this approximation, successive maxima of the $\delta\vec{u}$'s and $\delta\vec{r}$'s appear to be causally related, whether they actually are or not. This last statement is based on the following argument. After averaging over the directions of the $\delta\vec{u}$'s and $\delta\vec{r}$'s, these quantities are distinguished from particle to particle only by their magnitudes. Now suppose that immediately before some time t particle i has the current maximum $\delta\vec{u}$, but at time t the $\delta\vec{u}$ of particle j, which is remote from and unconnected with particle i, becomes the new system maximum. If, as we assume in our approximation, the effect of all the parameters involved in a collision (other than the magnitudes of the $\delta\vec{u}$'s and $\delta\vec{r}$'s) is fairly regular from collision to collision, then the $\delta\vec{u}$ in the collision that produces the new maximum at time t must be of the same order of magnitude as the old maximum $\delta\vec{u}_i$. There is in effect a relation between these $\delta\vec{u}$'s because they are distinguished only by their magnitudes. Hence, the new maximum $\delta\vec{u}_j$ is effectively related to the old maximum $\delta\vec{u}_i$.

Experimentally, the assumption of regularity does turn out to be a moderately good one. This can be seen most easily from the $\log_{10} D_p$ curves in Figures 3 through 11. There are fluctuations, of course, but in general, the jumps in these curves are reasonably regular.

In sum so far, we have argued that in order to find the overall exponentiation rate, it is only necessary to calculate the maximum $\delta\vec{u}$ and $\delta\vec{r}$ in the system and that these maxima are in effect causally related to their past. We now make one additional postulate which will allow these maxima to be calculated:

Postulate 2. The particle having the maximum $\delta\vec{u}$ and $\delta\vec{r}$ at time t is the one which has effectively undergone the most collisions up to time t.

The term "effectively" is used in Postulate 2 because the particle with the maximum $\delta\vec{u}$ and $\delta\vec{r}$ need not actually have undergone the most collisions. For instance in our previous example, after the 3-4 collision particle 4 has undergone only one collision but effectively has undergone all of the collisions in the sequence (as well as whatever collisions preceded the 1-2 collision).

Postulate 2 is simply the statement that the particle with the largest $\delta\vec{u}$ and $\delta\vec{r}$ is most likely to be the one which has undergone the most collisions because collisions are the mechanism for increasing the $\delta\vec{u}$'s and $\delta\vec{r}$'s.

We can now solve Eqs. (127) for the system maximum $\delta\vec{u}$ and $\delta\vec{r}$ by taking n in those equations to be the index n* that counts collisions in the sequence which has the maximum collision rate. We must also take τ in these equations to be the time τ* between the collisions counted by n*. At each collision in this maximum sequence, the resulting $\delta\vec{u}$'s (and $\delta\vec{r}$'s) of the two particles are approximately equal in magnitude and are therefore both system maxima. By Postulate 2, however, we shall assume that the one of these two which undergoes the earliest succeeding collision is the maximum in which we are interested; the other of these two particles will be ignored in our approximation.

In the solution of Eqs. (127), we shall obtain second-order difference equations in the $\delta\vec{u}$'s and $\delta\vec{r}$'s. These equations necessarily involve two successive collisions in the maximum sequence. There are

two distinct ways in which the two collisions can occur. Suppose that particle i is the maximum in the first collision between i and j and that one of i and j then goes on to collide with k. We then have the possible sequences (i-j, i-k) and (i-j, j-k). In the first case, Eqs. (127a) and (127b) apply to both collisions; in the second case Eqs. (127c) and (127d) apply to the first collision, and Eqs. (127a) and (127b) to the second collision. But it can be shown that the same second-order equations result in either case; therefore, for definiteness we consider the (i-j, i-k) sequence and solve Eqs. (127a) and (127b).

We define $\delta\vec{u}_{n*}$ and $\delta\vec{r}_{n*}$ to be the maxima we are following in the maximum sequence. In order to avoid unwieldy notation, we now drop the * from n* until stated otherwise. As in Eqs. (94) through (97), we use δx_n and δz_n for the components of $\delta\vec{r}_n$ and $\delta\vec{u}_n$ along $\hat{u}_n$ and δy_n and δw_n for the components of $\delta\vec{r}_n$ and $\delta\vec{u}_n$ along $\hat{b}_n$. We also define ξ_n to be the angle measured from $\hat{b}_n$ to $\hat{b}_{n+1}$ (on the maximum collision sequence):

$$\hat{b}_{n+1} = R(\xi_n)\hat{b}_n \ . \tag{128}$$

With the help of the first line of Eq. (67), we may write

$$P_n\delta\vec{u}_n = \delta z_n\hat{u}_n - \delta w_n\hat{b}_n \ , \tag{129a}$$

$$P_n\delta\vec{r}_n = \delta x_n\hat{u}_n - \delta y_n\hat{b}_n \ . \tag{129b}$$

Now take the dot product of $\hat{b}_{n+1}$ with both sides of Eqs. (127a) and (127b), and use Eqs. (128) and (129); this gives

$$\delta w_{n+1} = \frac{1}{2} \{-[\sin \xi_n + \sin(\xi_n - \theta_n)]\delta z_n \tag{130a}$$

$$+ [\cos \xi_n - \cos(\xi_n - \theta_n)]\delta w_n\} - \frac{u_n \cos(\xi_n - \theta_n)}{d \sin \frac{\theta_n}{2}} \delta y_n \; ,$$

$$\delta y_{n+1} = \frac{1}{2} \{-[\sin \xi_n + \sin(\xi_n - \theta_n)]\delta x_n \tag{130b}$$

$$+ [\cos \xi_n - \cos(\xi_n - \theta_n)]\delta y_n\} + \tau^*_{n+1} \delta w_{n+1} \; ,$$

where τ^*_{n+1} is the time between collisions on the maximum sequence. We next average Eqs. (130) on the collision parameters ξ_n, u_n, θ_n, and τ^*_{n+1}; the averages are carried out in Appendix B and result in

$$\delta w_{n+1} = -\frac{1}{4} \delta w_n - \frac{u\pi}{4d} \delta y_n \; , \tag{131a}$$

$$\delta y_{n+1} = -\frac{1}{4} \delta y_n + \tau^* \delta w_{n+1} \; , \tag{131b}$$

where τ^* is the mean time between collisions of the maximum sequence and where u is the system average of u_n.

One would expect u in the maximum sequence to be larger than the average u, at first at least. However, experimentally the speeds of the particles with the maximum $\delta\vec{u}$ and $\delta\vec{r}$ were on the order of the mean particle speed, although the speeds were widely distributed. This may seem more reasonable in the light of the following argument: suppose the maximum $\delta\vec{u}$ is associated with a single particle throughout a long sequence of collisions. It is then reasonable to expect that particle to sample the velocity distribution fairly and to have an average speed

close to the system average. Conversely, suppose the maximum $\delta\vec{u}$ is associated with many different particles during a long sequence of collisions. In this case it is reasonable to expect the different particles also to represent the velocity distribution fairly. In either case, the average speed of the particles in the maximum sequence may reasonably be expected to be close to the system average; therefore, for collisions in the maximum sequence the average relative speed of one particle to the other may also be reasonably expected to be close to the system average relative speed u.

Eqs. (131) may now be solved in a manner identical to the solution of Eqs. (100) and (101). One obtains the same second-order equations for δw and δy:

$$\delta w_{n+2} + \frac{1}{2}\left(1 + \frac{\pi u_T \tau^*}{2d}\right)\delta w_{n+1} + \frac{1}{16}\,\delta w_n = 0 \ , \tag{132a}$$

$$\delta y_{n+2} + \frac{1}{2}\left(1 + \frac{\pi u_T \tau^*}{2d}\right)\delta y_{n+1} + \frac{1}{16}\,\delta y_n = 0 \ . \tag{132b}$$

These equations have the two independent solutions $(-1)^n e^{\gamma_+^* n}$ and $(-1)^n e^{\gamma_-^* n}$, where $\gamma_\pm^*$ is given by

$$\gamma_\pm^* = -\ln 4 \pm \cosh^{-1}\left(1 + \frac{\pi u_T \tau}{2d}\right) \tag{133}$$

Since we are interested only in the dilating space, we use the plus sign in Eq. (133) and write

$$\delta w_n = \delta w_0 (-1)^n e^{\gamma^* n} \ , \tag{134a}$$

$$\delta y_n = \delta y_0 (-1)^n e^{\gamma^* n} \ , \tag{134b}$$

where $\gamma*$ is defined by

$$\gamma* = \cosh^{-1}\left(1 + \frac{m u \tau}{2d}\right) - \ln 4 . \tag{135}$$

If one forms the dot product of $\hat{\vec{u}}_{n+1}$ with both sides of Eqs. (127a) and (127b), uses Eqs. (26), (128), and (129 , and averages on ξ_n, u_n, θ_n and τ_{n+1}, then one obtains (see Appendix B for averages)

$$\delta z_{n+1} = \frac{1}{4} \delta z_n , \tag{136a}$$

$$\delta x_{n+1} = \frac{1}{4} \delta x_n + \tau* \delta z_{n+1} . \tag{136b}$$

Eqs. (136) have the general solutions

$$\delta z_n = \delta z_0 \, e^{-n \ln 4} , \tag{137a}$$

$$\delta x_n = (\delta x_0 + 4 t_n \delta z_0) e^{-n \ln 4} , \tag{137b}$$

where t_n $(= n\tau*)$ is the time of the nth collision. The magnitudes $|\delta \vec{u}_n|$ and $|\delta \vec{r}_n|$ are dominated very quickly as n increases by δw_n and δy_n of Eqs. (134). Hence, $\gamma*$ of Eq. (135) is the exponentiation rate with respect to the index n $(= n*)$ in the maximum sequence; therefore, by Corollary 1b, $\gamma*$ is the exponentiation rate for D_q and D_p of Eqs. (16) and (17).

We now restore the * to n*, and we let n without a star count collisions for the average particle, that is, we let

$$n(t) = \frac{t}{\tau} , \tag{138}$$

where τ is the mean time between collisions for a single particle. Let β be the ratio of n* to n, so we have

$$n*(t) = \beta n(t) \ . \tag{139}$$

But by the definition of τ* and n*, we must also have

$$n*(t) = \frac{t}{\tau*} \ , \tag{140}$$

and hence we obtain, from Eqs. (138) through (140),

$$\tau* = \frac{\tau}{\beta} \ . \tag{141}$$

As mentioned, according to Corollary 1b we have

$$D_p = D_{po} \ e^{\gamma* n*} \ , \tag{142a}$$

$$D_q = D_{qo} \ e^{\gamma* n*} \ . \tag{142b}$$

Next define γ so that

$$D_p = D_{po} \ e^{\gamma n} \ , \tag{143a}$$

$$D_q = D_{qo} \ e^{\gamma n} \ . \tag{143b}$$

Then from Eqs. (135) and (139) through (143), we see that

$$\gamma = \beta \left[\cosh^{-1}\left(1 + \frac{\pi u \tau}{2\beta d}\right) - \ln 4 \right] \ . \tag{144}$$

We now make a very crude argument that β is given in order of

magnitude by

$$\beta \approx \ln N . \qquad (145)$$

Observe an N-particle system for one mean collision time τ. During this time, each particle undergoes one collision on the average; thus, from Eq. (139), β collisions occur in the maximum sequence. At any instant during this time, there is precisely one particle in the system that not only has the maximum $\delta\vec{u}$ and $\delta\vec{r}$ but also is in the maximum sequence. (There are two particles with the maximum $\delta\vec{u}$ and $\delta\vec{r}$, but only one of these is in the maximum sequence.) Now add one particle to the system and suppose that during the time τ the only change is that the new particle collides once with some other particle. If the new particle happens to collide with the particle with maximum $\delta\vec{u}$ and $\delta\vec{r}$ in the maximum sequence, then, by the supposition that nothing else changes, there will be $\beta+1$ collisions in the maximum sequence during the time τ; otherwise, there will be β collisions in the maximum sequence. Assuming that the new particle has the probability $1/N$ of colliding with any particular particle, we find the expected average increase in β for an increase from N to N+1 particles to be $1/N$, which leads to Eq. (145).

We prefer to let Eq. (144) stand without substituting for β because Eq. (145) was obtained by such a crude argument. In the later comparison of Eq. (144) to experiment, however, we shall use Eq. (145) for lack of a better calculation.

For comparison of γ of Eq. (144) to experimental quantities, observe from Eqs. (13) and (14) that we may write D_q and D_p as

$$D_p = D_{po} \, 10^{\lambda_p t} \, , \tag{146a}$$

$$D_q = D_{qo} \, 10^{\lambda_q t} \, . \tag{146b}$$

Thus, from Eqs. (138), (143), and (146) we have

$$\lambda_q = \lambda_p = \frac{\gamma}{\tau \ln 10} \, . \tag{147}$$

In actual comparison to experiment it will be convenient to write

$$\gamma = \lambda \tau \ln 10 \, , \tag{148}$$

where λ is the common value of λ_q and λ_p, and to compare the experimental evaluation of Eq. (148) to Eq. (144).

CHAPTER IV

RESULTS OF THE NUMERICAL EXPERIMENTS

Previously we gave only a rudimentary description of the numerical experiments; here we present the details of them and show our results. The procedure for choosing initial conditions to obtain a fair sample of the energy surface is described, the macroscopic characteristics of the system are discussed, and the computer parameters are compared to data for a real gas. After these preliminaries the central point of this chapter is reached in setting forth the quantitative findings. Finally, the error in the numerical method and its consequences in the empirical results are considered.

Initial Conditions

To determine values for the statistical quantities λ_q and λ_p of Eqs. (13) and (14) with any degree of certainty, one requires a reasonable sampling of the energy surface for each set of macroscopic conditions. It is apparent from the number of degrees of freedom involved that an exhaustive sample would be prohibitively time-consuming. We therefore base our sampling procedure on the fact that empirically our system is a C-system, and hence almost all trajectories sample the entire energy surface.

Several original sets of initial conditions were selected by taking the coordinates and momenta from a table of random numbers. Experiments were run with these conditions, and occasionally during the

course of an experiment the coordinates and momenta as they existed at the time were saved to be used subsequently as initial conditions in further experiments. In turn, these further experiments produced sets of initial conditions for still further experiments, and so on. Thus, a fair sample was obtained on the basis of the stochastic properties of a C-system trajectory.

Error in the integration process also added to the randomness of the sample. The effect of error was that each integration step displaced the system point somewhat from the true trajectory. The distance from the true trajectory presumably increased exponentially within the energy surface as the system evolved; thus, error introduced early in the process could grow quite large after long integration times. The farther a point became in time from the initial point along a numerically integrated trajectory, the better that point was from the point of view of a random sample. Of course, this had to be accounted for when the error in experimentally observed quantities was estimated, as will be discussed later.

Whether the source of initial conditions was random numbers or previous experiments, they were processed in initiating each experiment as we now describe. The given initial conditions were taken to be those of the unprimed system. The coordinates were uniformly scaled to reach the desired density, and any particles closer together than $.9\sigma$ were separated to this distance. The total linear momentum was reduced to zero by subtracting $1/N$ times the total momentum from the momentum of each particle. The angular velocity of the system was found by applying the inverse of the inertia tensor to the total angular momentum. The

angular momentum was reduced to zero by adding the negative of the angular velocity to the system as a whole. The linear momenta were then uniformly scaled to attain the desired total energy. At this point, if the initial conditions were derived from a random number table, the system was integrated until an approximately Maxwellian velocity distribution was obtained. Finally, the initial conditions for the primed system were derived from those of the unprimed one by making small displacements (about 10^{-8} per particle in the units of Eq. (8)) in the unprimed coordinates and momenta.

Comparison to a Real Gas

The physical reality of the gas model of Eq. (7) can perhaps be seen more easily than otherwise by expressing the macroscopic system parameters in a standard system of units. For this purpose, we chose neon as a basis of computation. By use of the atomic mass and the tabulated[16] Lennard-Jones parameters ϵ and σ for this gas, one can convert the computer units of Eq. (8) to, say, MKS units. We have made this conversion; the results are given in Table 1. We use k_B for the Boltzmann constant and the abbreviations m.u., l.u., t.u., and e.u. for the computer units of mass, length, time, and energy, respectively. For comparison, we also give the values of the particle mass m and the Lennard-Jones parameters ϵ and σ in the table.

During the following discussion of the experimental results, we use Table 1 to express quantities in familiar units whenever it serves to elucidate the physical state of the computer model.

Table 1. Conversion Between Computer and MKS Units for Neon.

Quantity	Computer Units	MKS Units
Mass	1 m.u.	3.34×10^{-26} kgm
Length	1 l.u.	2.74×10^{-10} meter
Time	1 t.u.	1.12×10^{-12} sec
Energy	1 e.u.	2.00×10^{-21} joule
k_B (Boltzmann Constant)	$.00690 \dfrac{\text{e.u.}}{\text{°K-particle}}$	$1.38 \times 10^{-23} \dfrac{\text{joule}}{\text{°K-particle}}$
m (Particle Mass)	1 m.u.	3.34×10^{-26} kgm
σ	1 l.u.	2.74×10^{-10} meter
ϵ	.25 e.u.	5.00×10^{-22} joule

Tabulation of Quantitative Results

The majority of the computer experiments were run at approximately constant temperature. The quantitative results of these are given in Table 2. Except as noted otherwise, all of the tabulated quantities are given in computer units (cf. Table 1). Each of these experiments was performed with $N = 100$.

The first entry in Table 2 is the number density ρ, given in particles per unit area. For comparison of experimental states to states of a real gas, the fraction of the liquid-neon density that ρ represents is given second in the table. Third, we give the temperature T in degrees Kelvin. For this purpose, T in the table is calculated as the time average of the instantaneous temperature defined by

$$ T = \frac{1}{N\,k_B} \sum_{i=1}^{N} \frac{1}{2}\,m\,v_i^2 \,, \qquad (149) $$

where v_i is the speed of the ith particle. Because the system of our experiments is isolated, the energy remains constant, and the temperature fluctuates.[1] However, in our experiments the standard deviation of the instantaneous temperature from the tabulated time average, as calculated from step to step in the integration process, had a mean value of about .6 per cent averaged over all the experiments (the maximum deviation in any one experiment was 2.2 per cent). Therefore, we consider the temperature as given to be a well-defined thermodynamic variable of the system.

The next two entries of Table 2 are the experimental values for λ_p and λ_q of Eqs. (13) and (14). These are the slopes of the straight

Table 2. Quantitative Results of the Numerical Experiments at
          Approximately Constant Temperature.

ρ	$\%$ liq ρ	$T(°K)$	λ_p	λ_q	λ	2B	3B	4B	W	t_r	τ	Y_{exp}
.1200	14.8	327	.935	1.09	1.01	64	9	2	88	2.14	1.22	2.83
.1000	12.3	312	.857	.882	.870	148	19	2	192	6.20	1.62	3.23
.0800	9.84	310	.705	.704	.704	182	10	0	202	9.84	2.44	3.95
.0800	9.84	303	.666	.685	.676	178	17	1	215	9.56	2.22	3.46
.0600	7.38	300	.690	.705	.697	91	5	0	101	6.15	3.05	4.89
.0600	7.38	300	.646	.675	.660	130	7	0	144	8.70	3.02	4.59
.0600	7.38	305	.791	.830	.810	123	7	1	140	7.15	2.55	4.76
.0400	4.92	297	.501	.522	.511	136	7	0	150	14.0	4.67	5.49
.0400	4.92	290	.504	.507	.505	129	5	0	139	13.9	5.00	5.82
.0200	2.46	294	.353	.358	.355	76	2	0	80	18.6	11.6	9.51
.0200	2.46	295	.557	.559	.558	64	2	0	68	13.9	10.2	13.1
.0100	1.23	290	.252	.257	.255	40	0	0	40	16.0	20.0	11.7
.0080	.984	290	.203	.206	.205	62	0	0	62	33.8	27.3	12.8
.0080	.984	290	.200	.200	.200	72	0	0	72	35.2	24.4	11.3
.0060	.738	290	.177	.183	.180	50	1	0	52	36.2	34.8	14.4
.0060	.738	290	.232	.232	.232	52	0	1	55	32.4	29.5	15.7
.0040	.492	290	.157	.162	.159	48	0	1	51	43.5	42.7	15.6
.0040	.492	290	.112	.119	.116	49	0	0	49	56.4	57.6	15.3
.0040	.492	289	.146	.157	.152	42	0	0	42	44.7	53.2	18.6
.0020	.246	290	.102	.102	.102	36	0	0	36	68.0	94.4	22.1
.0010	.123	290	.052	.054	.053	28	0	0	28	100	179	21.9
.0008	.098	290	.056	.065	.060	23	0	0	23	98.0	213	29.4
.0008	.098	290	.080	.087	.084	16	0	0	16	69.0	216	41.5
.0008	.098	290	.051	.056	.053	23	0	0	23	112	245	29.9
.0004	.049	290	.040	.042	.041	12	0	0	12	100	418	39.1
.0004	.049	290	.038	.046	.042	12	0	0	12	100	418	40.0
.0004	.049	290	.018	.022	.020	14	0	0	14	172	616	28.2
.0002	.025	290	.055	.059	.057	10	0	0	10	99.6	498	65.2
.0002	.025	290	.025	.027	.026	19	0	0	19	214	562	33.8
.0001	.012	290	.025	.030	.027	4	0	0	4	99.7	1247	78.7
.0001	.012	290	.014	.015	.014	5	0	0	5	315	3150	104
.0001	.012	290	.019	.020	.019	13	0	0	13	269	1036	46.2

lines resulting from a least-squares fit of the logarithm plots, as mentioned earlier. In Figures 3 through 11 we show some typical examples of these plots with the fitted straight lines superposed on them. In these figures, $\log_{10}D_p$ and the corresponding fitted line are plotted as solid curves while $\log_{10}D_q$ and its corresponding line are plotted as broken curves.

In view of Eq. (147), we expect λ_q to be equal to λ_p. As can be seen from the plots and from Table 2, this expectation is borne out to a surprising degree on consideration of the statistical fluctuations possible in such quantities. From this point, then, we drop the distinction between λ_q and λ_p and use the mean value λ as given next in Table 2 in all further calculations.

Following the λ's, we have tabulated the number of two-body, three-body, and four-body collisions, and a weighted sum W of these collisions, under the respective headings 2B, 3B, 4B, and W. No collisions of more than four particles were observed to occur.

In the weighted total W, three-body and four-body collisions were given the weights of two and three binary collisions. These weights represent the simplest sequences of binary collisions that would replace the multiple ones if the theoretical, hard spheres were to replace the experimental particles which have the Lennard-Jones interaction. One chooses the simplest sequences because it can be argued that these represent the true binary collision effects of a multiple collision, whereas more complicated sequences represent effects of higher order for which our simple theoretical model has no hope of an explanation. Thus, for the purpose of comparison to our theoretical results, we take W to
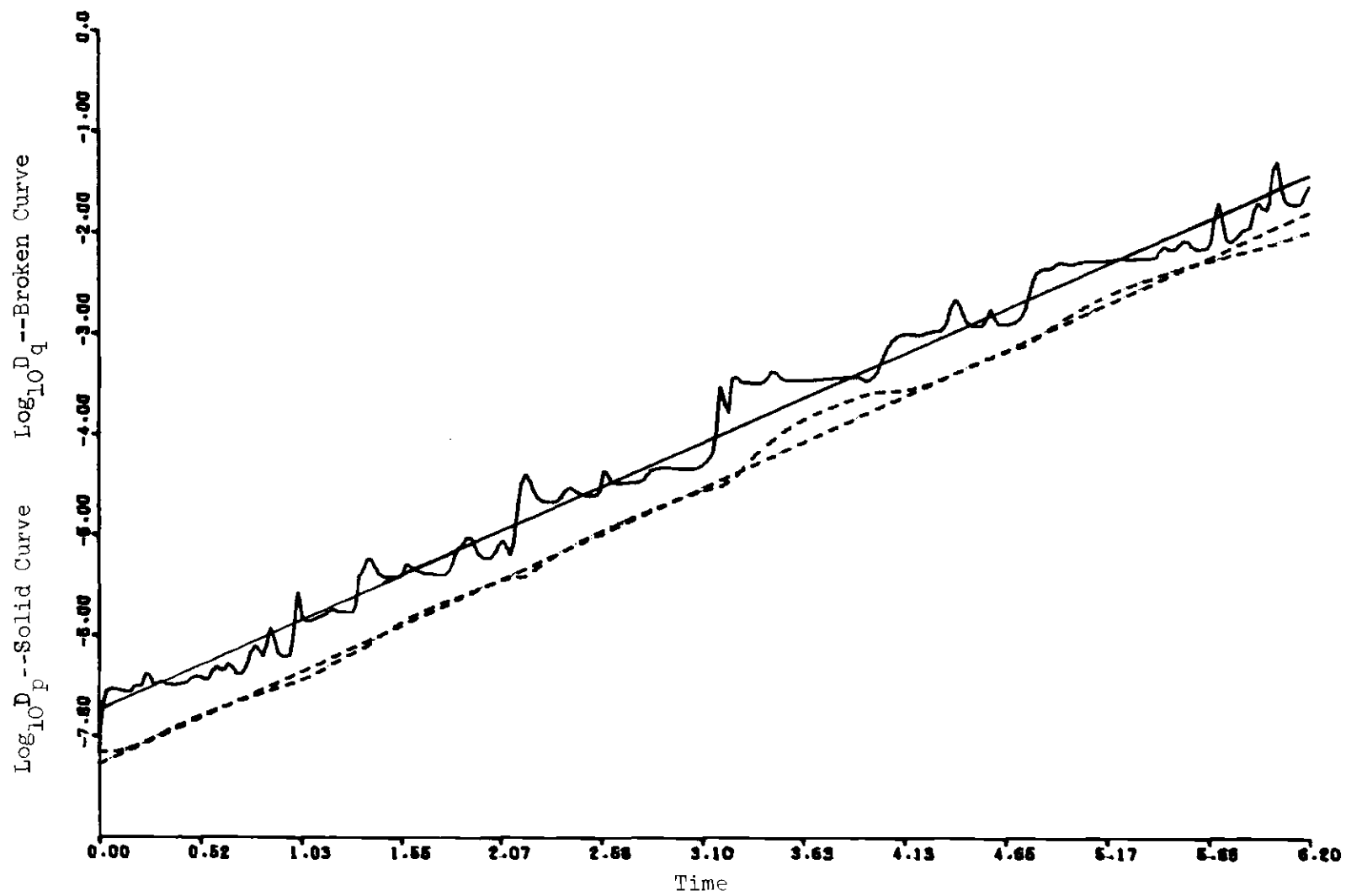
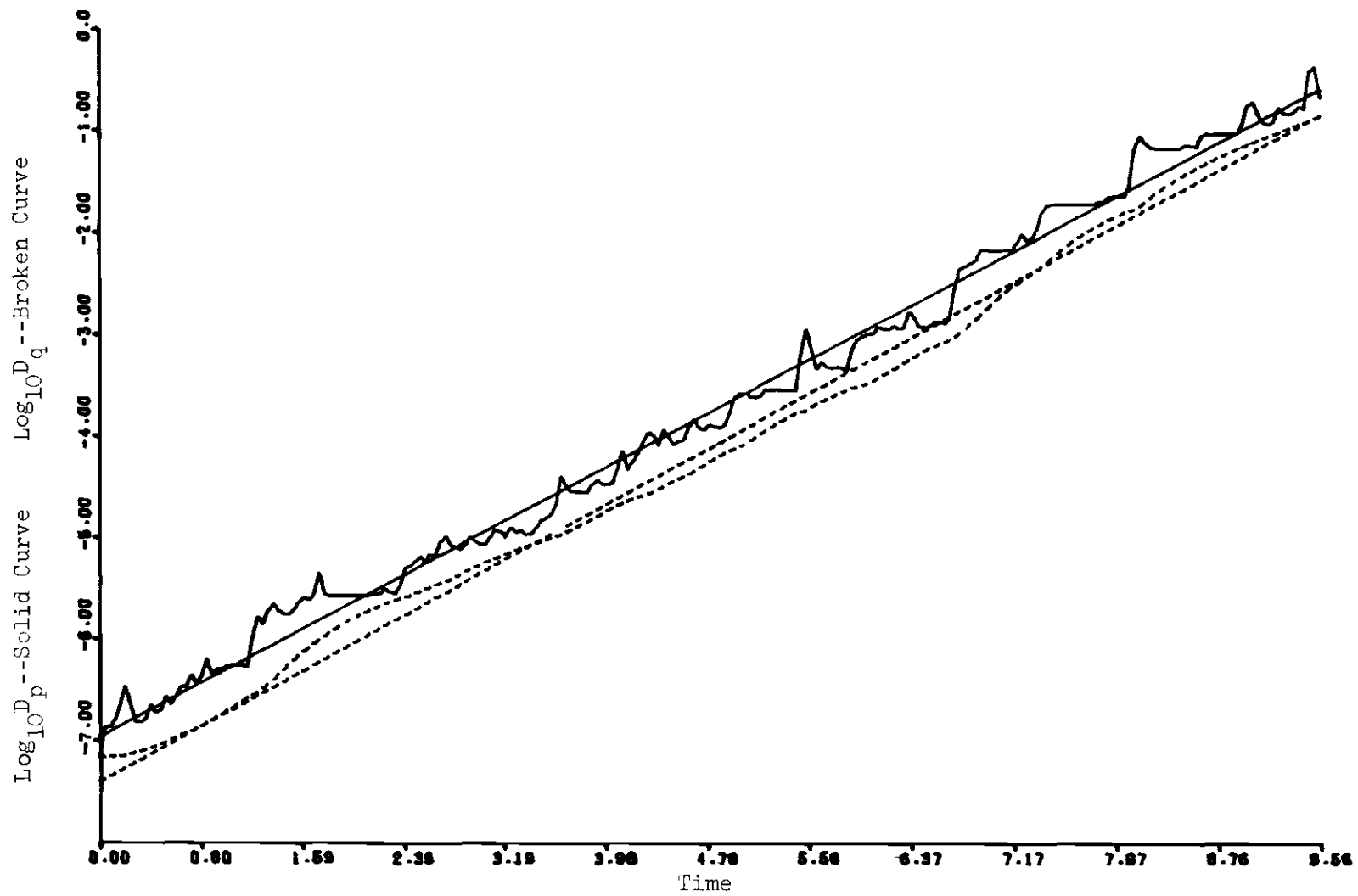Figure 3.   Plot of Data Corresponding to Entry 2 of Table 2.

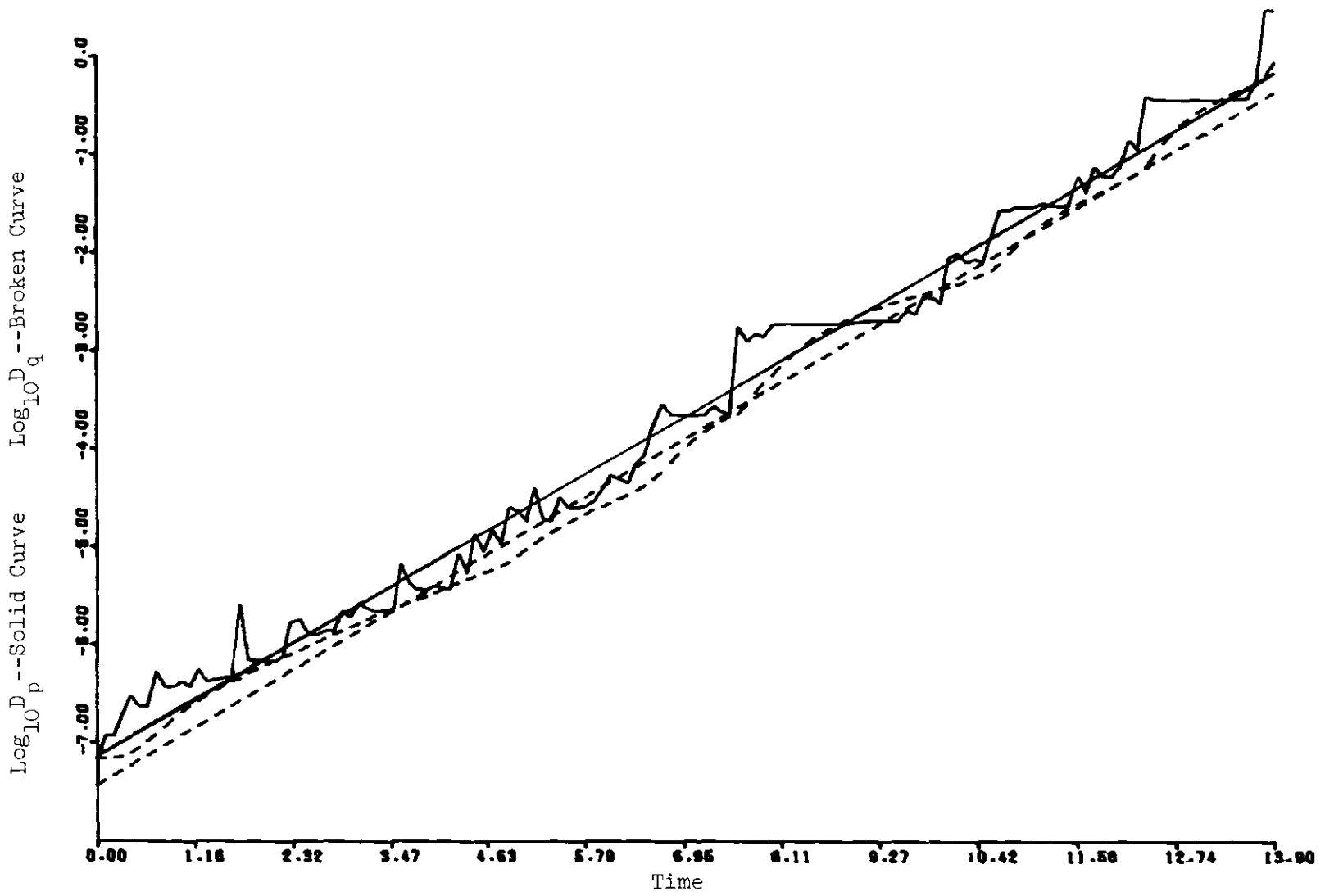Figure 4.   Plot of Data Corresponding to Entry 4 of Table 2.

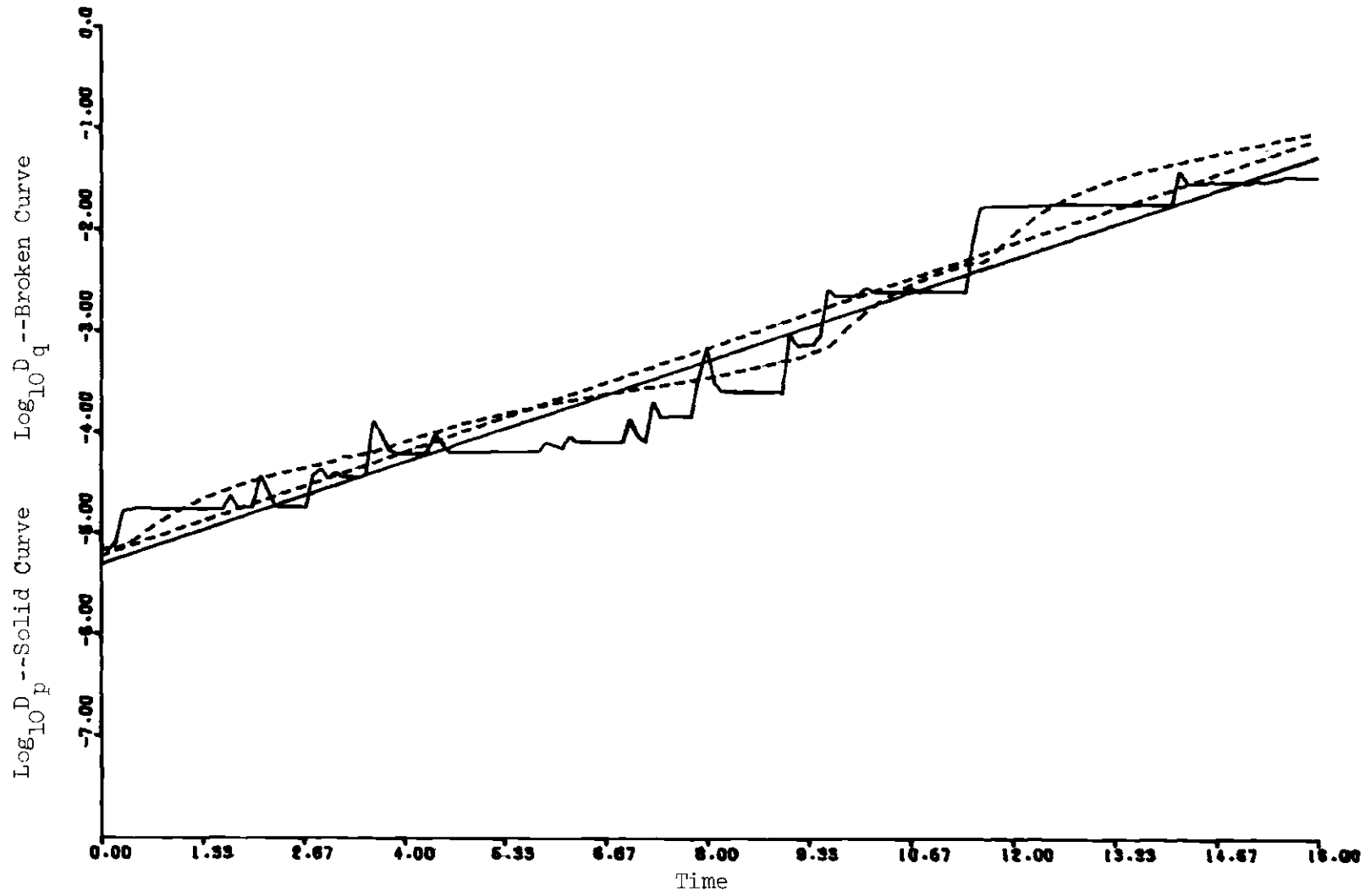Figure 5. Plot of Data Corresponding to Entry 9 of Table 2.

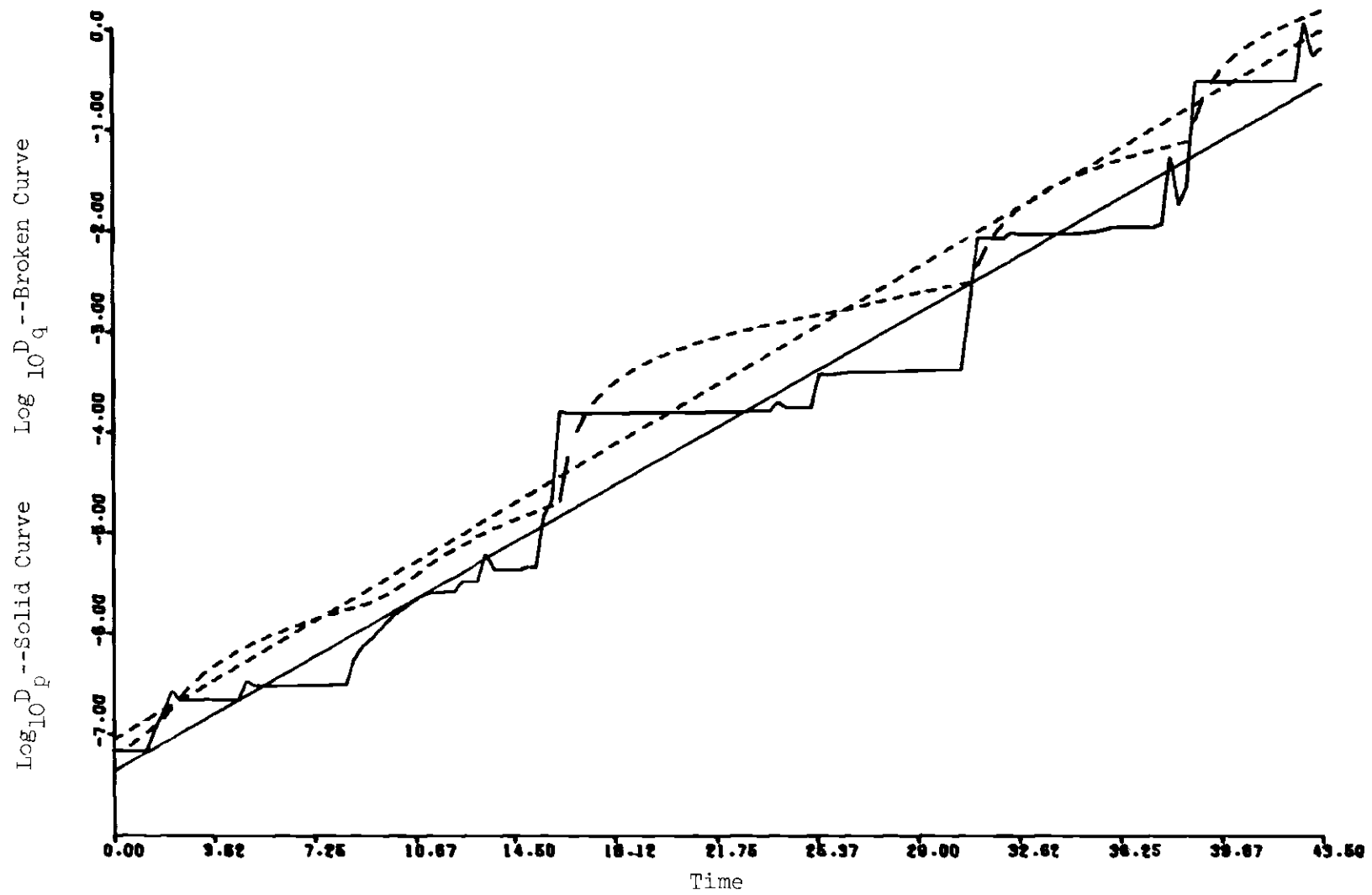Figure 6. Plot of Data Corresponding to Entry 12 of Table 2.

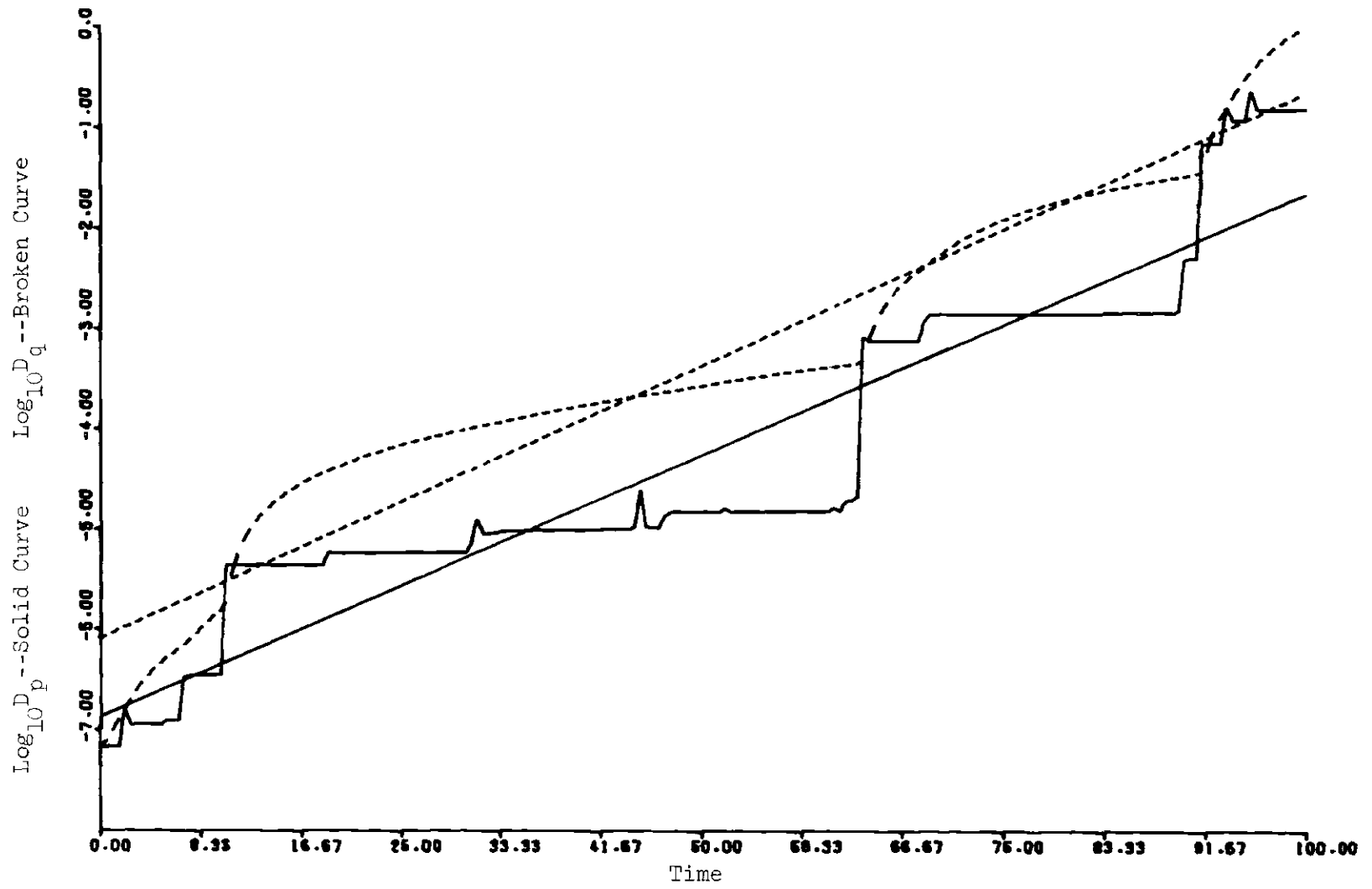Figure 7. Plot of Data Corresponding to Entry 17 of Table 2.

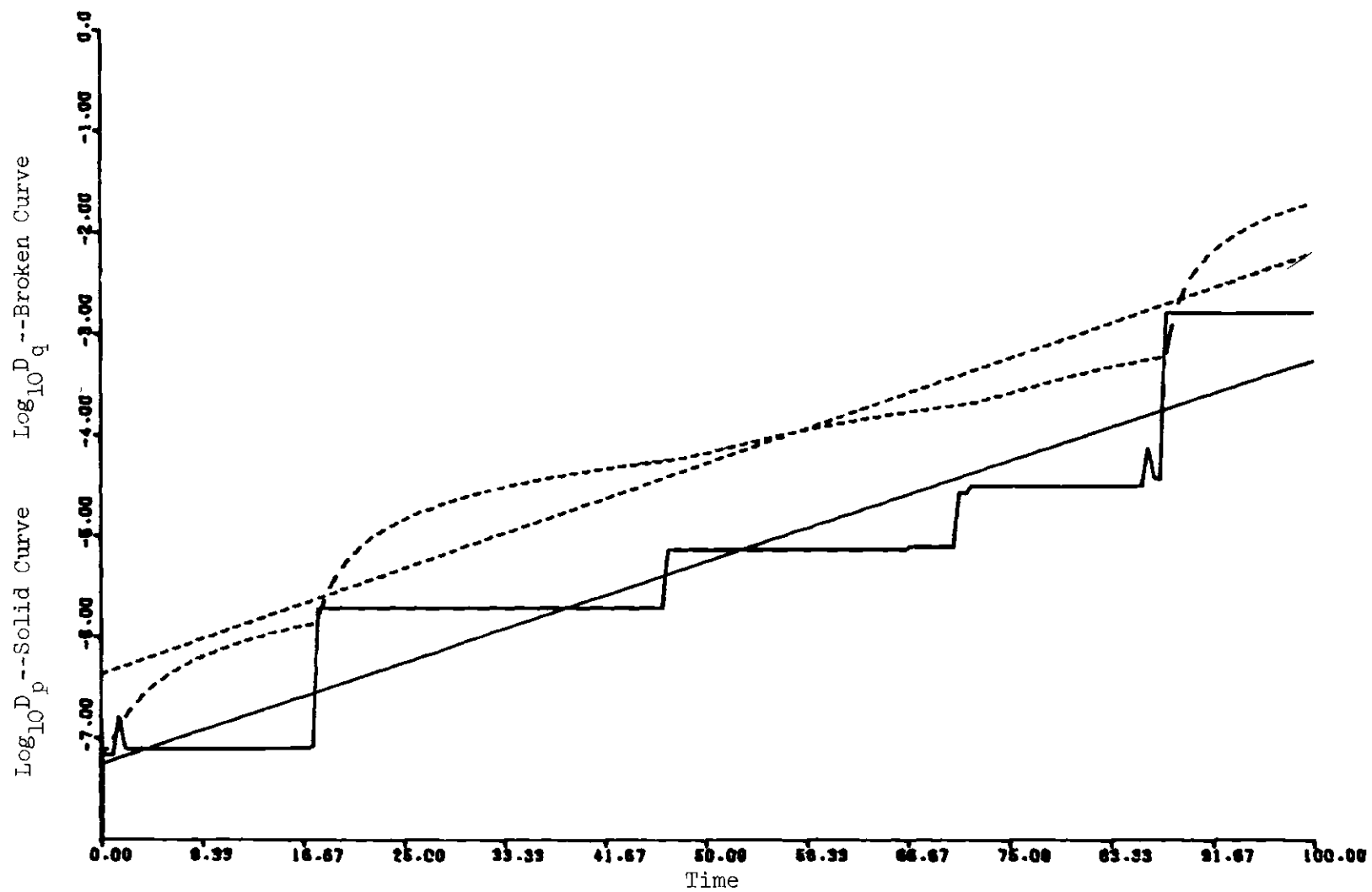Figure 8. Plot of Data Corresponding to Entry 21 of Table 2.

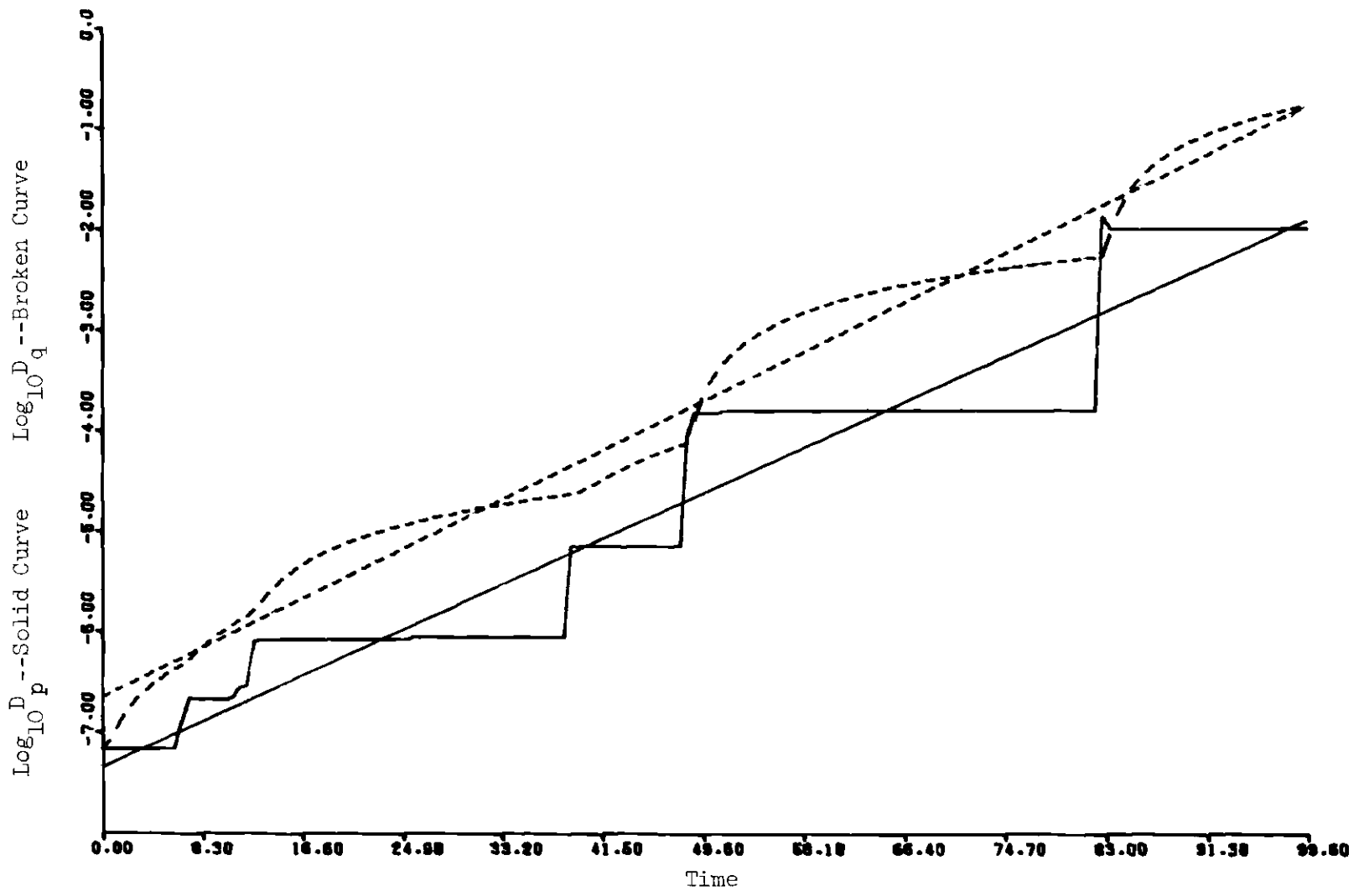Figure 9. Plot of Data Corresponding to Entry 25 of Table 2.

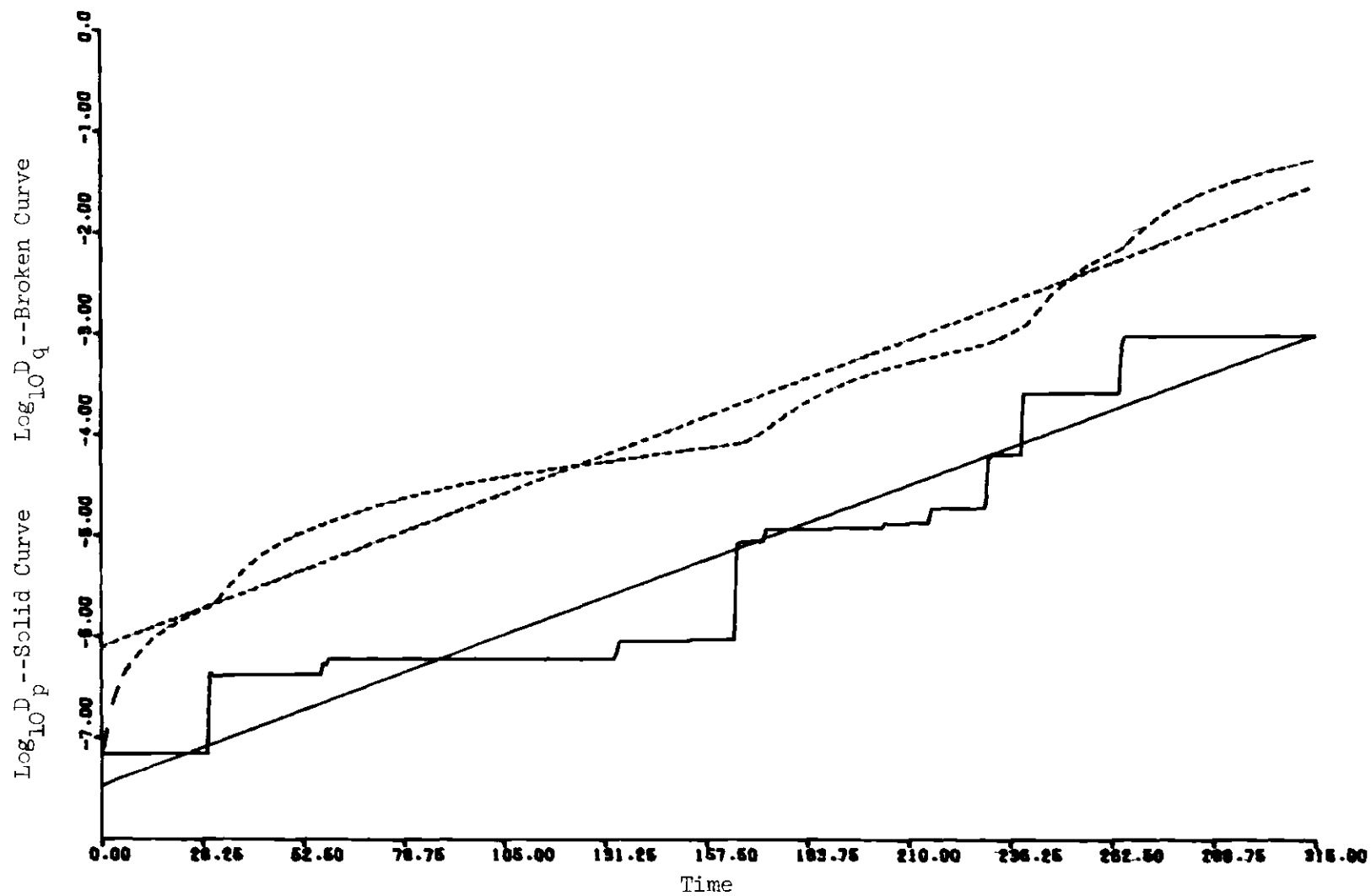Figure 10. Plot of Data Corresponding to Entry 28 of Table 2.

Figure 11. Plot of Data Corresponding to Entry 31 of Table 2.

be the total number of collisions occurring in an experiment and make
our theoretical comparison as if all collisions were binary ones.

After the collision data in Table 2, we give the duration of
each experiment t_r. By comparison of these values with Table 1, one
sees that even our longest experiments are of extremely short duration
on a macroscopic scale--a few tenths of a nanosecond at most. With t_r
and W, we can calculate the effective mean time τ between collisions ac-
cording to

$$\tau = \frac{N}{2} \frac{W}{t_r} ,$$
(150)

where the factor of $N/2$ is included to obtain the mean time between col-
lisions of a single particle. These results are tabulated following t_r
in Table 2.

The experimental values γ_{exp} for the exponentiation rate are cal-
culated from Eq. (154) and are given after τ in Table 2. These results
are shown graphically in Figure 12, where γ_{exp} versus τ is plotted.

The results of a few experiments made holding the density con-
stant and varying the temperature are given in Table 3. Table 3 has the
same format as Table 2. The first line of Table 3 is copied for refer-
ence from the twelfth line of Table 2.

Table 4 shows the evaluation of β of Eq. (139) from data taken in
some preliminary experiments. From left to right, the Table 4 entries
are the number of particles N, the total number of collisions observed,
the average number n of collisions per particle, the number n* of col-
lisions in the maximum sequence, β as calculated from Eq. (139), and
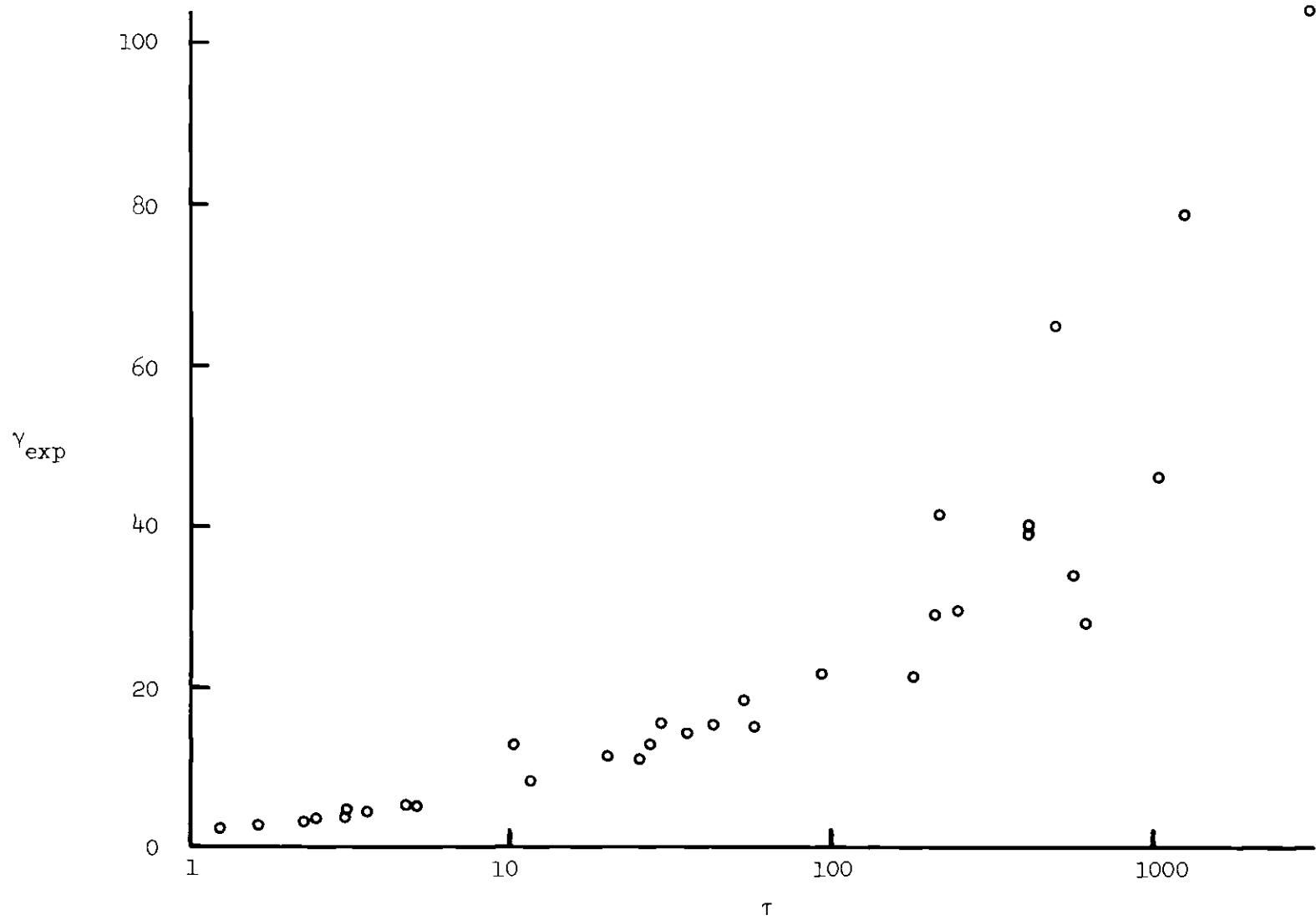
Figure 12. Experimental γ Versus τ.

Table 3. Quantitative Results of the Numerical Experiments at Constant Density. The first line of this table is copied from Table 2, Line 12.

ρ	$\%$ liq ρ	$T(^\circ K)$	λ_p	λ_q	λ	2B	3B	4B	W	t_r	τ	γ_{exp}
.0100	1.23	290	.252	.257	.255	40	0	0	40	16.0	20.0	11.7
.0100	1.23	435	.420	.440	.430	40	0	0	40	10.1	12.6	12.5
.0100	1.23	580	.460	.400	.430	23	0	0	23	6.00	13.0	12.9
.0100	1.23	725	.410	.430	.420	40	0	0	40	11.3	14.1	13.7

Table 4. Experimental Values of β Compared to Ln N for Small Systems.

N	Total Collisions	n	n*	β	$\dfrac{\beta}{\ln N}$
8	172	21.5	50	2.33	1.12
12	232	19.3	48	2.48	1.00
16	152	9.5	27	2.84	1.02
20	114	5.7	24	4.21	1.41

finally, the ratio of β to ln N. From this last entry, it appears that Eq. (145) is a reasonable (although slightly small) order-of-magnitude estimate for β for N in this range.

Accuracy

In our calculations the energy and linear momentum were conserved to one part in 10^8, but for such unstable systems, the conservation of energy (or momentum) is not a good accuracy test because these systems are not unstable in the direction normal to the energy surface. Thus, the error in the energy is additive from integration step to step, whereas the error introduced within the energy surface in a given step grows exponentially in succeeding steps. Furthermore, it is difficult to obtain an accurate error estimate for the Runga-Kutta[17] integration method used. Therefore, we adopted a reversed-integration procedure for error analysis.

For simplicity in this section, we shall plot the quantity $\log_{10}D$, where D is defined by

$$D = \sqrt{D_q^2 + D_p^2} \ . \tag{151}$$

Although D is dimensionally inhomogeneous, in view of the equality of λ_q and λ_p of Table 2 Eq. (151) is useful for illustrative purposes.

A pair of systems were integrated over a time period, and $\log_{10}D$ was plotted as shown in Figure 13 (solid curve). We shall call this the forward integration. The velocities were reversed in the final conditions of the forward integration, and these reversed conditions were used as initial conditions for a similar integration over the same time

period. The $\log_{10}D$ curve of this reversed integration is also shown in Figure 13 (broken curve).

The following discussion shows how these two integrations may be used to estimate the error. At the end of the forward integration the difference vector between the two systems has components in each of the dilating and contracting spaces. The dilating component is overwhelmingly the largest; the contracting component consists only of error introduced in the last few integration steps because contracting components in the initial conditions or introduced by earlier errors have decayed away exponentially by this time. Reversing the velocities interchanges the dilating and contracting components;[18] so the dilating component of the reversed integration initially consists only of error from the forward integration. During the reversed integration the dilating component grows, and the initially large contracting component decays exponentially. When the dilating component exceeds the contracting one, the $\log_{10}D$ curve turns upward. The upward-turned part thus results entirely from the exponentiation of the initial error plus error accumulated during the reversed integration itself. On the other hand, the $\log_{10}D$ curve of the forward integration results from exponentiation of the initial difference between the systems. On a logarithmic plot, the distance of the forward curve above the upward-turned part of the reversed curve measures the ratio of the initial difference to the error.

The ratio $\log_{10}D$ on the forward curve to $\log_{10}D$ on the reversed curve can be computed from the data for Figure 13. This computation yields a geometric mean of 2.0 for the ratio, the largest and smallest values of the individual ratios in the average being 3.2 and .6,
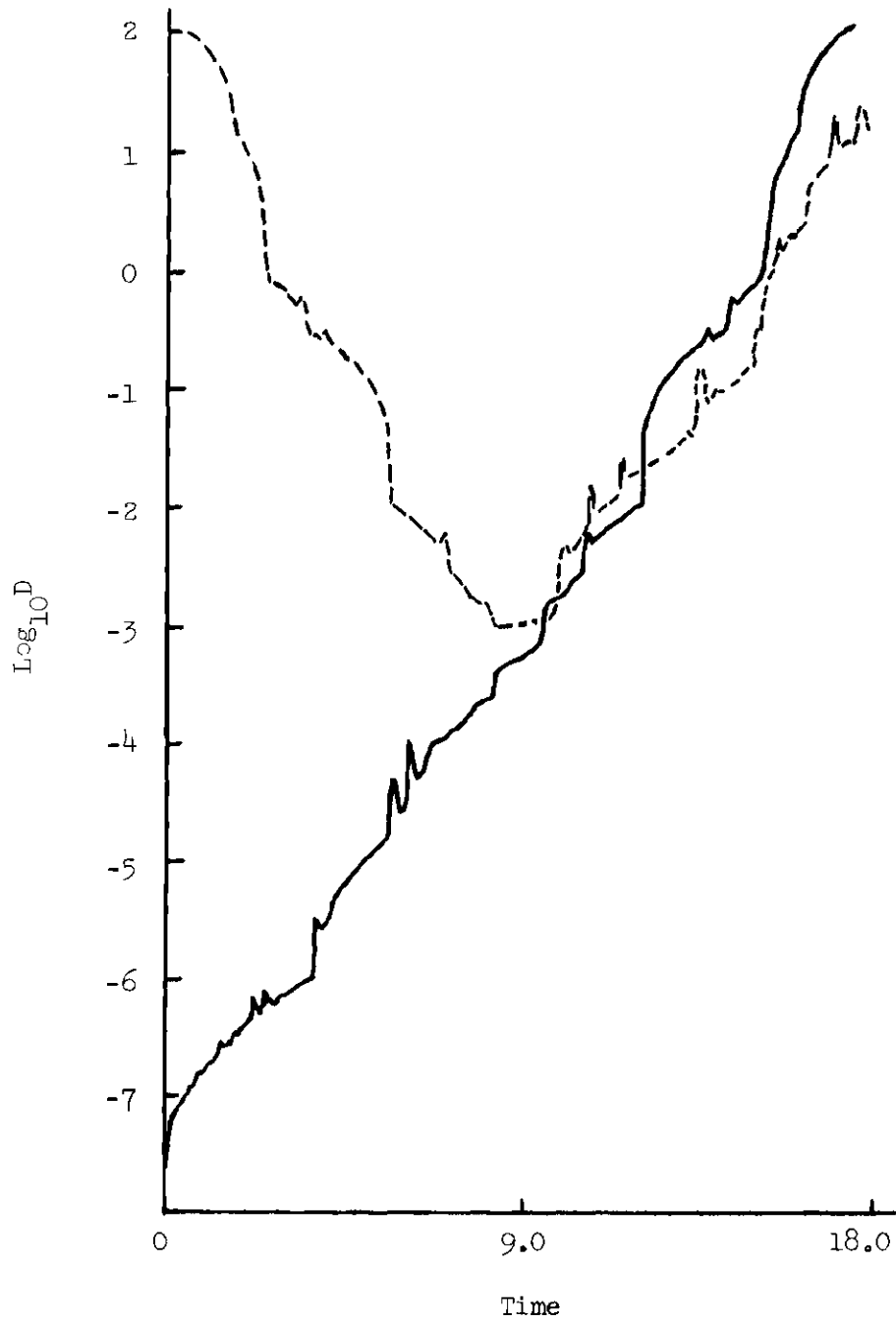
Figure 13. Plot of $Log_{10}D$ versus Time for Forward (Solid Curve) and Reversed (Broken Curve) Integrations.

respectively. Hence, the error in the distance D between the two system points is approximately 50 per cent in the early points of the integration, and we shall assume that this value holds for D_p and D_q separately.

The 50 per cent figure is not a good estimate for the error in λ_p and λ_q, however, because the early error does not propagate into later data points in a random fashion but rather exponentiates regularly. The $\log_{10}D_p$ and $\log_{10}D_q$ plots may be shifted up or down, but the over-all slope is only affected by the random error introduced into each point. The ratio of D_p and D_q to the random error increases exponentially with time, since there is no reason for errors in each system to depend on the distance between systems. Therefore, except for the early data points, the integration error is negligible, and even the early error tends to change the vertical intercepts but not the slopes of the least-squares-fitted lines. Hence, integration error is unlikely to be significant in the experimental values of λ_p and λ_q.

We have yet to consider errors introduced in the least-squares fitting process. Although it is possible to compute a so-called correlation factor for such a fit, it is difficult to interpret and, further-more, would be affected by deviations from straight-line behavior that can be accounted for on a dynamical basis, namely, the discontinuities in the $\log_{10}D_p$ plots and the rapid increase in the $\log_{10}D_q$ curves immedi-ately after a jump in D_p (see Figures 3 through 11). We feel, there-fore, that the best idea of the accuracy of the fitting process can be obtained graphically, and we refer the reader to Figures 3 through 11, which are typical.

CHAPTER V

EXPERIMENTAL AND THEORETICAL COMPARISON

We have already pointed out one feature of the theory that is verified experimentally: the exponentiation rates are the same in configuration and momentum space. In this chapter, we compare other theoretical quantities to the experimental results of the preceding chapter.

A question naturally arises about the applicability of the hard-sphere theory to the Lennard-Jones experiment. This question is complicated by the uncertainties in the theoretical solution. Fortunately, one can make an independent argument to arrive at the temperature dependence of γ in the hard-sphere case. Comparison of this result to the experimental data indicates that the hard-sphere model is a moderately good one for the experimental system.

Temperature Dependence

The temperature dependence of γ for hard-spheres may be inferred from the following argument: consider a hard-sphere system as in our previous theoretical discussion. Hold N and the volume constant and let the temperature T, as defined by Eq. (149), vary. Since the total energy E is entirely kinetic in this case, T does not fluctuate. Suppose we have two trajectories $y_1(t) = (\vec{r}_{i1}(t), \vec{p}_{i1}(t))$ and $y_1'(t) = (\vec{r}_{i1}'(t), \vec{p}_{i1}'(t))$ at temperature T_1 such that $D_{q_1}(t)$ and $D_{p_1}(t)$, defined as indicated by Eqs. (11) and (12), have the average time behavior given by

$$\langle D_{q_1}(t) \rangle = D_{oq_1} \; e^{\lambda_1 t} \; , \tag{152a}$$

$$\langle D_{p_1}(t) \rangle = D_{op_1} \; e^{\lambda_1 t} \; , \tag{152b}$$

where the brackets indicate average behavior over the trajectories.

Further, consider two similar trajectories y_2 and y_2' which belong to systems at temperature T_2 and which are related to y_1 and y_1' at $t = 0$ by

$$\vec{r}_{i2}(0) = \vec{r}_{i1}(0) \; , \tag{153a}$$

$$\vec{p}_{i2}(0) = \zeta \; \vec{p}_{i1}(0) \; , \tag{153b}$$

$$\vec{r}'_{i2}(0) = \vec{r}'_{i1}(0) \; , \tag{153c}$$

$$\vec{p}'_{i2}(0) = \zeta \; \vec{p}'_{i1}(0) \; , \tag{153d}$$

where ζ is defined by

$$\zeta = \sqrt{\frac{T_2}{T_1}} \; . \tag{154}$$

From hard-sphere dynamics and the initial conditions of Eqs. (153), it follows that

$$\vec{r}_{i2}(t) = \vec{r}_{i1}(\zeta t) \; , \tag{155a}$$

$$\vec{p}_{i2}(t) = \zeta \; \vec{p}_{i1}(\zeta t) \; , \tag{155b}$$

with similar equations holding for the primed trajectories. Thus, one has that the distances $D_{q_2}(t)$ and $D_{p_2}(t)$, defined as in Eqs. (11) and (12), are related to $D_{q_1}(t)$ and $D_{p_1}(t)$ by

$$D_{q_2}(t) = D_{q_1}(\zeta t) \, , \tag{156a}$$

$$D_{p_2}(t) = \zeta \, D_{p_1}(\zeta t) \, . \tag{156b}$$

Therefore, if we write the average time behavior of $D_{q_2}(t)$ and $D_{p_2}(t)$ as

$$\langle D_{q_2}(t) \rangle = D_{oq_2} e^{\lambda_2 t} \, , \tag{157a}$$

$$\langle D_{p_2}(t) \rangle = D_{op_2} e^{\lambda_2 t} \, , \tag{157b}$$

then from Eqs. (152), (156), and (157), we obtain

$$\lambda_2 = \zeta \, \lambda_1 \, . \tag{158}$$

The collision exponentiation rates γ_1 and γ_2 may be found, in analogy with Eq. (148), to be given by

$$\gamma_1 = \lambda_1 \tau_1 \, , \tag{159a}$$

$$\gamma_2 = \lambda_2 \tau_2 \, , \tag{159b}$$

where τ_1 and τ_2 are the mean times between collisions for a single particle in the systems of temperatures T_1 and T_2, respectively. In

terms of γ_1 and γ_2, Eqs. (152) and (157) may be rewritten as

$$\langle D_{q_1} \rangle = D_{oq_1}\, e^{\gamma_1 n_1}\ , \tag{160a}$$

$$\langle D_{p_1} \rangle = D_{op_1}\, e^{\gamma_1 n_1}\ , \tag{160b}$$

$$\langle D_{q_2} \rangle = D_{oq_2}\, e^{\gamma_2 n_2}\ , \tag{160c}$$

$$\langle D_{p_2} \rangle = D_{op_2}\, e^{\gamma_2 n_2}\ , \tag{160d}$$

where n_1 and n_2 are the average collisions per particle in the systems at temperatures T_1 and T_2 respectively. From Eqs. (155) we have that

$$\tau_1 = \zeta\, \tau_2 \tag{161}$$

and, with the help of Eq. (171), that

$$\gamma_1 = \gamma_2\ . \tag{162}$$

Thus, the exponentiation rate with respect to collisions is independent of temperature for hard spheres. Since the hard-sphere system is ergodic and mixing,[2,12] this conclusion, which was arrived at by considering a time-averaged behavior, is applicable to the phase-averaged γ of Eq. (144). The combination $u\tau$ in Eq. (144) is proportional to the mean free path and hence is independent of temperature.

For the experimental system, one would expect γ to have only a small temperature dependence if the hard-sphere model is a good one for

it. That this is so can be seen from Table 3 where γ_{exp} varies only a few per cent over a wide temperature range.

By the above argument we have verified another of the theoretical conclusions and gained some confidence that the hard-sphere results apply to the experiments.

Dependence of γ on τ

The theoretical and experimental dependence of γ on τ will now be compared. Originally we set out to find the dependence of γ on the density ρ, but τ arises naturally in both the theoretical and experimental calculations and is the natural independent variable to use. Finding the dependence of γ on ρ would require knowing τ as a function of ρ. This function would have to be empirically determined at the densities involved, and having ρ as the independent variable offers no particular advantage for our purposes.

The average u of Eq. (144) is evaluated in Appendix C to be

$$u = \sqrt{2\pi}\ v_{RMS}\ , \tag{163}$$

where v_{RMS} is obtained from Eq. (149) according to

$$v_{RMS} = \sqrt{\frac{2k_B T}{m}}\ . \tag{164}$$

Since the particle diameter was taken to be σ in the experimental collision-counting process, we assign d in Eq. (144) to be given by

$$d = \sigma\ , \tag{165}$$

which is unity in the computer units of Table 1. Finally, we use

Eq. (145) with N = 100 as an estimate of the value of β, which yields

$$\beta \approx 4.6 \ . \tag{166}$$

With Eqs. (163) through (166), we can plot a theoretical γ vs τ

curve from Eq. (144); this curve is shown in Figure 14 superposed on the

data points from Figure 12. The fractional absolute deviation A of

this curve from the data points, given by

$$A = \frac{|\gamma_{exp} - \gamma|}{\gamma_{exp}} \ , \tag{167}$$

where γ is the theoretical value corresponding to γ_{exp}, has a mean value

of 21 per cent. In view of the range of τ covered and the estimates and

approximations made to obtain Eq. (144), this is extremely good agree-

ment. The discrepancies between the curve and experimental points for

the large τ values should perhaps be given a relatively small weight

because Postulate 1 used in deriving the theoretical γ is least likely

to be true for these points. This is because initially the $\vec{\delta u}$'s and

$\vec{\delta r}$'s are equal for all the particles, in direct contradiction to Postu-

late 1 at t = 0, and several collisions are necessary for the conditions

of this postulate to be established. The large-τ experimental points

which involve small numbers of collisions (say 10 or less) are therefore

the points least likely to satisfy Postulate 1.

Cooperative Behavior

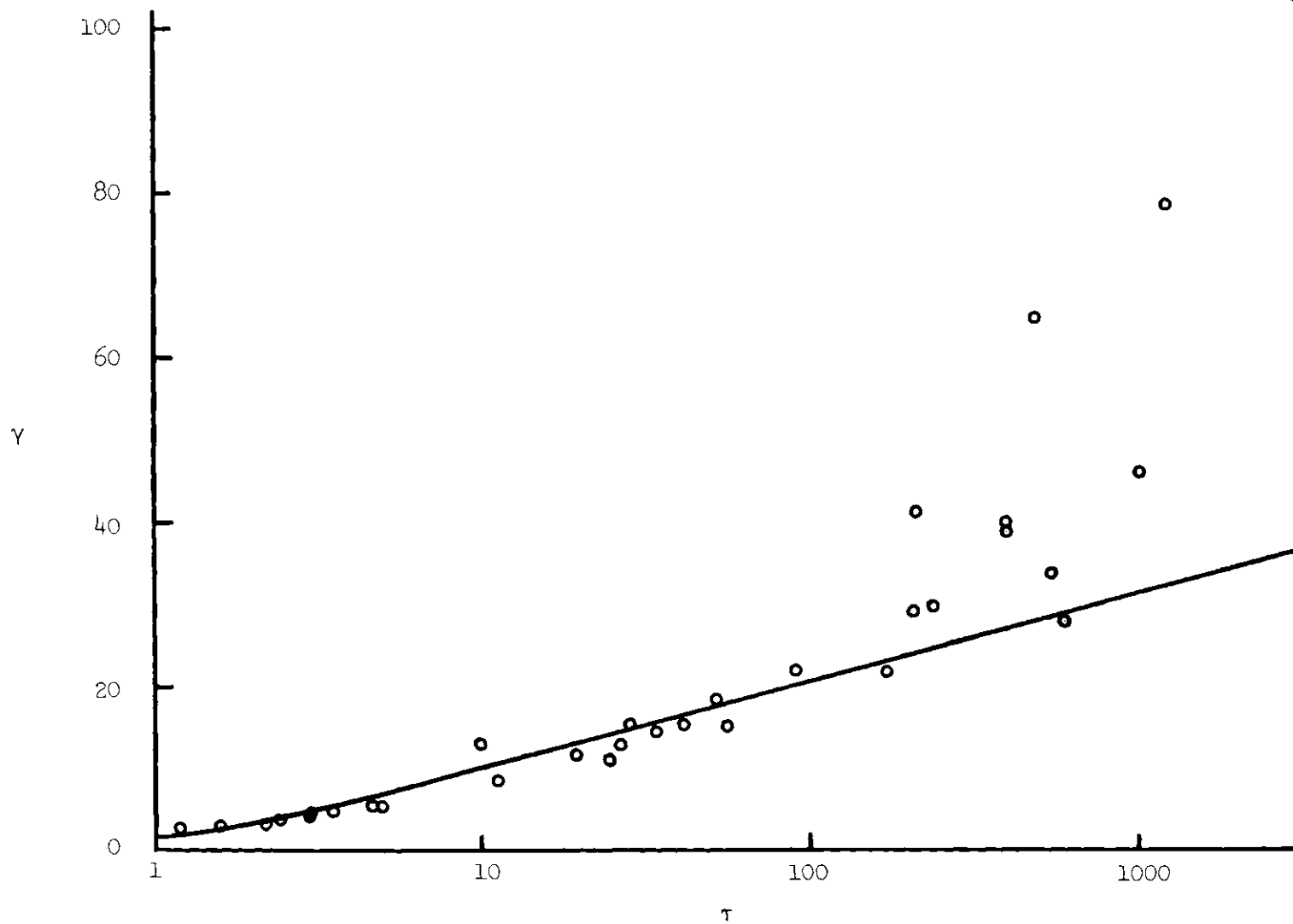The exponentiation rate (calculated as in Eq. (148)) for

Figure 14. Comparison of Theoretical and Experimental γ.

gravitational systems was reported by Miller[13] to be proportional to
the number of particles for N in the range 4-32. From this Miller con-
cluded that the long range of the gravitational force caused the system
to behave cooperatively, as if all N particles were tightly coupled.
In the density range observed in our experiments, however, the empiri-
cal exponentiation rate is in reasonably good agreement with the theo-
retical calculation which includes no such tight coupling and which
does not produce γ proportional to N (cf. Eq. (144)).

In two-dimensional systems, the three-body collision term is the
first divergent one in the calculation of transport coefficients.[3]
Because our data includes up to 15 per cent three-body and four-body
collisions in the high-density range, one would think that if coopera-
tive effects were to appear (as indicated by an increase in the experi-
mental γ over the theoretical one at high density), they would have done
so.

Thus, our results indicate that the divergences in the transport
coefficients are probably not due to the sudden appearance of coopera-
tive behavior. Experiments at somewhat higher densities would be
required to make a definitive statement on this point.

Summary and Conclusions

The problem treated by Boltzmann and Gibbs involved developing a
workable theory for irreversible and equilibrium thermodynamic behavior
starting from reversible microscopic dynamics.[1,4-7] In developing the
theory, the so-called ergodic assumption was introduced which asserts,
loosely speaking, that the trajectory for an isolated system samples
the entire energy surface. This assumption and the statistical

mechanics based on it gave rise to mathematical problems which are extremely difficult. Only recently has it been shown that the ergodic assumption is true for a hard-sphere gas. This was done by Sinai,[2,12] who proved that trajectories of a hard-sphere gas separate exponentially in time and that this property is sufficient to guarantee the validity of the Boltzmann-Gibbs ergodic assumption.[2] Sinai's result is believed to be extendable to a large class of systems with purely repulsive forces,[11] but there is some doubt regarding the possibility of extending it to systems having attractive forces.

A Lennard-Jones system, which has attractive forces, was studied in the research reported here. A series of computer experiments were performed which provided strong empirical evidence that the trajectories of the Lennard-Jones system separate exponentially in time. Therefore, to computer accuracy, this system satisfies the ergodic assumption.

The computer experiments just mentioned also lend themselves to the testing of an hypothesis in the field of kinetic theory. In kinetic theory, divergences appear when transport coefficients are calculated by series expansion in the density.[3] This calculation assumes that binary collisions are the dominant transport mechanism at low density, with three-body, four-body, etc., collisions becoming important sequentially as the density is increased. It was thought possible that this sequential assumption might be erroneous and that cooperative behavior-- collisions among large numbers of particles--might suddenly appear as the density increased.

To test this hypothesis, a theory of trajectory-exponentiation in a hard-sphere gas was developed. This theory yielded a rate for the

exponentiation which represented only non-cooperative phenomena because only binary collisions were considered. For the density and temperature range observed in the experiments, the empirically observed exponentiation was in reasonable agreement with the theory. This agreement extended to densities high enough to make it unlikely that divergences in the transport coefficients are due to cooperative behavior.

APPENDIX A

We want to show that Eqs. (108) and (109) reduce to Eqs. (112) and (113) with the approximations of Eqs. (110) and (111).

Eq. (109) averages over the ensemble as

$$\langle \delta y_{n+2} \rangle = - \left\langle \left[1 + \frac{2u\tau_{n+2}}{d \sin \frac{\theta_{n+1}}{2}} + \frac{\tau_{n+2}}{\tau_{n+1}} \right] \delta y_{n+1} \right\rangle \tag{A1}$$

$$- \left\langle \frac{\tau_{n+2}}{\tau_{n+1}} \delta y_n \right\rangle \,.$$

From Eq. (109), we also see that δy_{n+1} is independent of τ_{n+2} and θ_{n+1}, and further, that δy_n is independent of τ_{n+1} as well. Thus from Eq. (A1) we have

$$\langle \delta y_{n+2} \rangle = - \left\langle 1 + \frac{2u\tau_{n+2}}{d \sin \frac{\theta_{n+1}}{2}} \right\rangle \langle \delta y_{n+1} \rangle \tag{A2}$$

$$- \left\langle \frac{\tau_{n+2}}{\tau_{n+1}} \right\rangle \langle \delta y_n \rangle - \left\langle \frac{\tau_{n+2}}{\tau_{n+1}} \delta y_{n+1} \right\rangle \,.$$

We now take Eq. (109) for δy_{n+1}, multiply it by τ_{n+2}/τ_{n+1}, and average the result, with the fact in mind that δy_n and δy_{n-1} are independent of τ_{n+1}, to obtain

$$\left\langle \frac{\tau_{n+2}}{\tau_{n+1}} \delta y_{n+1} \right\rangle = - \langle \tau_{n+2} \rangle \left\{ \left\langle \frac{1}{\tau_{n+2}} \right\rangle \langle \delta y_n \rangle \right. \tag{A3}$$

$$+ \frac{1}{<\tau_{n+1}>} \left\langle \left(\frac{2u\tau_{n+1}}{d\sin\frac{\theta_n}{2}} + \frac{\tau_{n+1}}{\tau_n} \right) \delta y_n \right\rangle$$

$$+ \left\langle \frac{\tau_{n+1}}{\tau_n} \delta y_{n-1} \right\rangle \Bigg\} \quad .$$

In Eq. (A3), we use the approximation of Eq. (111) to replace $1/<\tau_{n+1}>$ by $<1/\tau_{n+1}>$, which results in

$$\left\langle \frac{\tau_{n+2}}{\tau_{n+1}} \delta y_{n+1} \right\rangle = \left\langle \frac{\tau_{n+2}}{\tau_{n+1}} \right\rangle \Bigg\{ \left\langle - \left[1 + \frac{2u\tau_{n+1}}{d\sin\frac{\theta_n}{2}} + \frac{\tau_{n+1}}{\tau_n} \right] \delta y_n \right\rangle \qquad (A4)$$

$$- \left\langle \frac{\tau_{n+1}}{\tau_n} \delta y_{n-1} \right\rangle \Bigg\} \quad .$$

On comparison of Eq. (A4) with Eq. (A1), we see that

$$\left\langle \frac{\tau_{n+2}}{\tau_{n+1}} \delta y_{n+1} \right\rangle = \left\langle \frac{\tau_{n+2}}{\tau_{n+1}} \right\rangle <\delta y_{n+1}> \quad . \qquad (A5)$$

Substitution of Eq. (A5) into Eq. (A2) then yields

$$<\delta y_{n+2}> = - \left\langle 1 + \frac{2u\tau_{n+2}}{d\sin\frac{\theta_{n+1}}{2}} + \frac{\tau_{n+2}}{\tau_{n+1}} \right\rangle <\delta y_{n+1}> \qquad (A6)$$

$$- \left\langle \frac{\tau_{n+2}}{\tau_{n+1}} \right\rangle <\delta y_n> \quad .$$

It is consistent with the approximation of Eq. (111) to put

$$\left\langle \frac{\tau_{n+2}}{\tau_{n+1}} \right\rangle = 1 \; . \tag{A7}$$

With Eq. (A7), Eq. (A6) reduces to Eq. (113), which was to be shown.

An exactly analogous calculation allows Eq. (112) to be derived by averaging Eq. (108) and using the approximation of Eq. (110).

APPENDIX B

It is required to calculate the averages necessary for Eqs. (112), (113), (131), and (136). In this appendix, all center-of-mass quantities will be understood to be for particle i.

Consider a sequence of collisions $(i-j, i-k)$ which are numbered n and $n + 1$. Collision n has the velocity $\vec{u}_n$ in the center-of-mass frame given by

$$\vec{u}_n = \vec{u}_{i,n} - \vec{u}_{j,n} \; , \tag{B1}$$

and collision $n + 1$ has the velocity

$$\vec{u}_{n+1} = \vec{u}_{i,n+1} - \vec{u}_{k,n+1} \; , \tag{B2}$$

where the notation of Eq. (73) is used. From Eqs. (22) and (69), we have that

$$\vec{u}_{i,n+1} = \frac{\vec{u}_{i,n} + \vec{u}_{j,n}}{2} + R(\theta_n) \frac{(\vec{u}_{i,n} - \vec{u}_{j,n})}{2} \; . \tag{B3}$$

Hence, $\vec{u}_{n+1}$ may be written as

$$\vec{u}_{n+1} = \frac{\vec{u}_{i,n} + \vec{u}_{j,n}}{2} - \vec{u}_{k,n+1} + R(\theta_n) \frac{(\vec{u}_{i,n} - \vec{u}_{j,n})}{2} \; . \tag{B4}$$

From Eqs. (26) and (128) we see that

$$\hat{u}_{n+1} = R(\xi_n)\hat{u}_n \; . \tag{B5}$$

From Eq. (B5), we obtain the following relation for any angle α:

$$\vec{u}_{n+1} \cdot [R(\alpha)\vec{u}_n] = u_{n+1} \, u_n \cos(\xi_n - \alpha) \; . \tag{B6}$$

With proper selection of α, all of the trigonometric functions of Eqs. (130) may be generated.

Eqs. (B1), (B4), and (B6) combine to yield

$$u_{n+1} \, u_n \cos(\xi_n - \alpha) = \frac{1}{2} \cos \alpha (u_{i,n}^2 - u_{j,n}^2) + u_{i,n} \, u_{j,n} \sin \alpha \sin \varphi$$

$$- \vec{u}_{k,n+1} \cdot [R(\alpha)(\vec{u}_{i,n} - \vec{u}_{j,n})]$$

$$+ \frac{\cos(\alpha - \theta_n)}{2} u_n^2 \; , \tag{B7}$$

where φ is the angle measured from $\vec{u}_{i,n}$ to $\vec{u}_{j,n}$:

$$\hat{u}_{j,n} = R(\varphi)\hat{u}_{i,n} \; . \tag{B8}$$

Now we assume that the impact parameter b is uniformly distributed from $-d$ to d. From Eq. (145), the distribution $f(\theta)$ of scattering angles can then be calculated as

$$f(\theta) = \frac{1}{4} \sin \frac{\theta}{2} \; , \tag{B9}$$

where θ ranges from zero to 2π. We further assume that the velocities $\vec{u}_{i,n}$, $\vec{u}_{j,n}$, and $\vec{u}_{k,n+1}$ have isotropic directional distributions and are entirely uncorrelated either among themselves or with the angle θ_n.

With the foregoing assumptions, one successively replaces α of

Eq. (B6) with 0, θ_n, $\pi/2$, and $(\theta_n + \pi/2)$ and averages the results over θ_n and the $\vec{u}$'s to obtain

$$<\cos \xi_n> = 0 , \tag{B10}$$

$$<\cos(\xi_n - \theta_n)> \approx \frac{1}{2} , \tag{B11}$$

$$<\sin \xi_n> = 0 , \tag{B12}$$

and

$$<\sin(\xi_n - \theta_n)> = 0 , \tag{B13}$$

where in Eq. (B11) the approximation

$$\left\langle \frac{u_n}{u_{n+1}} \right\rangle \approx 1 \tag{B14}$$

has been made.

Similarly, we can further find that

$$\left\langle \frac{u_n \cos(\xi_n - \theta_n)}{d \sin \frac{\theta_n}{2}} \right\rangle \approx \frac{u\pi}{4d} , \tag{B15}$$

where again the approximation of Eq. (B14) has been used, and that

$$\left\langle \frac{u_n \sin(\xi_n - \theta_n)}{d \sin \frac{\theta_n}{2}} \right\rangle = 0 . \tag{B16}$$

Eqs. (B10) through (B16) list all of the averages required for

Eqs. (131) and (136). In addition, for Eqs. (112) and (113) we require $\left\langle 1/\sin \frac{\theta_n}{2} \right\rangle$, which is calculated from Eq. (B9) as

$$\left\langle \frac{1}{\sin \frac{\theta_n}{2}} \right\rangle = \frac{\pi}{2} \quad . \tag{B17}$$

APPENDIX C

Our objective is to compute the expectation value of u given in Eq. (163).

We assume that the ensemble average of u can be replaced by the average of this quantity over the particles of a single system. We further assume that the particle velocities are independent and have the equilibrium, two-dimensional Maxwell distribution $B(\vec{v})$ given by

$$B(\vec{v}) = \frac{m}{2\pi k_B T} \exp\left(- \frac{m|\vec{v}|^2}{2k_B T}\right) . \tag{C1}$$

From Eq. (C1), it can be shown that the distribution $B(u_{ij})$ of differences u_{ij}, defined by

$$u_{ij} = |\vec{v}_i - \vec{v}_j| , \tag{C2}$$

where $\vec{v}_i$ and $\vec{v}_j$ are distributed according to Eq. (C1), has the form

$$B(u_{ij}) = \frac{mu_{ij}}{2k_B T} \exp\left(- \frac{mu_{ij}^2}{4k_B T}\right) . \tag{C3}$$

By direct calculation, one obtains from Eq. (C3) that

$$<u_{ij}> = \sqrt{\frac{4\pi k_B T}{m}} . \tag{C4}$$

LITERATURE CITED

1. D. ter Haar, Elements of Statistical Mechanics (Holt, Rinehart, and Winston, New York, 1954).

2. V. I. Arnold and A. Avez, Ergodic Problems of Classical Mechanics (Benjamin, New York, 1968).

3. M. H. Ernst, L. K. Haines, and J. R. Dorfman, Reviews of Modern Physics 41, 296 (1969). This article contains a comprehensive list of publications in the field of contemporary kinetic theory.

4. See, for example, K. Huang, Statistical Mechanics (Wiley, New York, 1963).

5. G. E. Uhlenbeck and G. W. Ford, Lectures in Statistical Mechanics (Cornell University Press, Ithaca, 1959).

6. J. W. Gibbs, Elementary Principles in Statistical Mechanics (Dover, New York, 1960).

7. P. and T. Ehrenfest, The Conceptual Foundations of Statistical Mechanics, (Cornell University Press, Ithaca, 1959).

8. A. I. Khinchin, Mathematical Foundations of Information Theory (Dover, New York, 1957).

9. A. I. Khinchin, Mathematical Foundations of Statistical Mechanics (Dover, New York, 1949)

10. P. R. Halmos, Lectures on Ergodic Theory (Chelsea, New York, 1956).

11. A. S. Wightman in Statistical Mechanics at the Turn of the Decade, E. D. G. Cohen, Ed. (Marcel Dekker, New York, 1971).

12. J. Ford, Advances in Chemical Physics 24, 155 (1973).

13. R. H. Miller, Astrophys. J. 140, 250 (1964).

14. H. Goldstein, Classical Mechanics (Addison-Wesley, Reading, 1950).

15. H. Eyring, J. Walter, and G. E. Kimball, Quantum Chemistry (Wiley, New York, 1944), pp. 351-355.

16. C. Kittel, Introduction to Solid State Physics (Wiley, New York, 1966), pp. 81-85.

VITA

Spotswood Douglas Stoddard was born on January 20, 1943 in Memphis, Tennessee. He attended public schools in Georgia and Virginia and entered the Georgia Institute of Technology in 1961. On his graduation in 1965 with a B.S. degree in Physics, he went to work for IBM as a systems engineer. In 1967 he returned to the Georgia Institute of Technology and received M.S. (1969) and Ph.D. (1973) degrees in the School of Physics.

He was married to Margaret Phyllis Haynie in 1963, and his daughter, Margaret Ann, was born in 1967.